

**An investigation of the zinc binding characteristics of the RING finger
domain from the human RBBP6 protein using heteronuclear NMR
spectroscopy**



Takalani Mulaudzi

A mini-thesis submitted in fulfilment of the degree of M.Sc. (Structural Biology) in the
Faculty of Science, University of the Western Cape

Supervisor: Dr D.J.R. Pugh

November 2007

Keywords

^{15}N -HSQC

^1H - ^{113}Cd -HSQC

Cadmium ion

Coordination

Expression

NMR

RBBP6

RING

Spectroscopy

Zinc ion



Abstract

An investigation of the zinc binding characteristics of the RING finger domain from the human RBBP6 protein using heteronuclear NMR spectroscopy

Takalani Mulaudzi

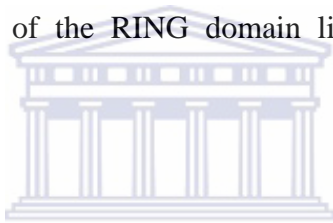
M.Sc. (Structural Biology) thesis, Department of Biotechnology, Faculty of Science, University of the Western Cape.

Retinoblastoma binding protein 6 (RBBP6) is a 250 kDa human splicing-associated protein that is also known to interact with tumour suppressor proteins p53 and pRb and to mediate ubiquitination of p53 via its interaction with Hdm2. RBBP6 is highly up regulated in oesophageal cancer, and has been shown to be a promising target for immunotherapy against the disease. RBBP6 is also known to play a role in mRNA splicing, cell cycle control and apoptosis.

RBBP6 contains a RING finger domain, a hallmark of E3 ubiquitin ligases, which is essential for its interaction with Hdm2. RING fingers are well-known structural motifs coordinating two zinc ions in a cross-braced manner by means of eight conserved cysteine or histidine residues. Sequence alignments suggest that the RBBP6 RING finger can be classified as a member of the U box family, which do not require zinc ions in order to fold, although they adopt the same structure as RING fingers, raising the question as to whether zinc is required in order for the RBBP6 RING to fold.

Previous analysis of a fragment of RBBP6 containing the RING finger domain showed that it contained an unstructured region at the N-terminus, which hampered efforts to investigate the protein using NMR. Here we report the truncation, expression and NMR analysis of two shortened RING constructs from which the unstructured region has been removed. Fragments shortened by 13 and 19 amino acids respectively were expressed as soluble GST-fusions and samples prepared for NMR analysis.

1D and 2D NMR showed that the longer of the two shortened constructs adopted the same fold as the original RING construct, whereas the shorter was unfolded, from which we deduce that the boundary of the RING domain lies between the two shortened constructs.



Using NMR we showed that zinc is required in order for the protein to fold, and that zinc ions can be replaced by cadmium ions without significantly disrupting the structure. Using 1D directly detected ^{113}Cd spectroscopy we were able to observe the cadmium ions bound into the protein, which to our knowledge, has never been done before for proteins. We were also able to observe coherence transfer between the cadmium ions and H^β protons in the side chains of the coordinating cysteine residues, which will be used in future work to identify the residues involved in coordinating the zinc ions.

Declaration

I declare that “*An investigation of the zinc binding characteristics of the RING finger domain from the human RBBP6 protein using heteronuclear NMR spectroscopy*” is my own work that has not been submitted for any degree or examination at any university and that all the sources I have used or quoted have been indicated and acknowledged by complete references.

Takalani Mulaudzi

November 2007



Signed.....

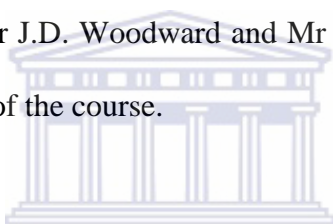
Dedication

I dedicate this work to my late father **Naledzani Jeffrey Mulaudzi**.



Acknowledgements

I would like to show my appreciation to my supervisor Dr D.J.R. Pugh and to Prof D.J.G Rees for giving me the opportunity to do this project in their laboratory. My special thanks go to my supervisor, Dr D.J.R. Pugh who for this guidance during the project and whom this thesis would have not has been possible. I am also grateful to Dr A. Atkinson and Miss Jean McKenzie for helping with many of the NMR experiments. For their scientific inputs, insights and technical assistance with the project, my thanks go to Mr A. Faro and Mr J.E. Onyemata. Many people have given support and technical insights into this project in the Biochemistry lab; I would like to give special thanks to the following people: Dr M. Meyer, Mr F. February, Mr A. Pretorius and Mr M Chibi. Finally, my thanks go to my classmates, Mr J.D. Woodward and Mr E.K. Murungi, for their support throughout the theoretical part of the course.



I would like to thank my fiancé Mr W.k. Masuku and my daughter Akhonamahle Felicity Masuku, for their patience and support when this project kept me away from them in their hour of need. I express my gratitude to my family: my mother Mrs M.J Ngwenya, my brother Mulalo Mulaudzi, my uncle Dr B.P. Maseko, and my cousin Dr L. Maseko for their family support.

I would like to thank the National Research Foundation of South Africa and the Carnegie Corporation for providing me with financial support.

List of tables and figures

Tables

Chapter 2

Table 2.1: Experimental set up for cloning PCR products into pGEM-T Easy vector.

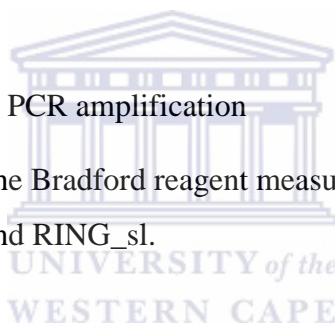
Table 2.2: Ligation reactions for cloning DNA fragments into pGEX-6P-2 expression vector.

Table 2.3: Experimental set up for restriction double digests of pGEM-T Easy and pGEX-6P-2 expression vector.

Chapter 3

Table 3.1: Primers used for PCR amplification

Table 3.2: Absorbance of the Bradford reagent measured at 595 nm for the standard protein (BSA) and RING_sl.



Figures

Chapter 1

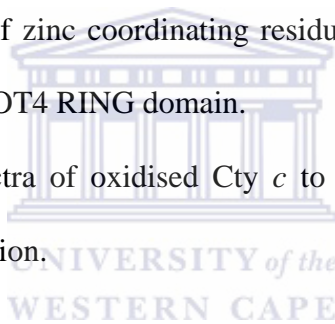
Figure 1.1: Schematic representations of the domain structure of RBBP6 homologues from different species.

Figure 1.2: Alignment of the RBBP6 RING finger against a number of RING fingers and RING finger-like domains.

Figure 1.3: Schematic representation of the zinc coordination in RING finger and PHD domains.

Figure 1.4: 3D Structure of the MAT1C3HC4 RING finger.

- Figure 1.5: Cartoon representation of a 3D structure of the PHD from the AIRE1 (PDB: 1XWH).
- Figure 1.6: The ubiquitin-proteasome pathway.
- Figure 1.7: Tetrahedral coordination found in RING finger proteins.
- Figure 1.8: RING-H2 domain from EL5 requires Zn^{2+} for folding.
- Figure 1.9: RING2 from HHARI requires Zn^{2+} in order to fold.
- Figure 1.10: Coordination of Zn^{2+} by cysteine residues.
- Figure 1.11: Determination of zinc coordinating residues by replacement of zinc with ^{113}Cd in the p44 RING domain.
- Figure 1.12: Determination of zinc coordinating residues by replacement of zinc with ^{113}Cd in the CNOT4 RING domain.
- Figure 1.13: ^{15}N HSQC spectra of oxidised Cty *c* to probe the residues involved in Zn/Cd coordination.



Chapter 3

- Figure 3.1: Primers used for PCR amplification of RING finger.
- Figure 3.2: 1% agarose gel electrophoresis showing PCR amplification of both shortened RING constructs.
- Figure 3.3: 1% agarose gel electrophoresis showing colony PCR screening for recombinant clones.
- Figure 3.4: 1% agarose gel electrophoresis showing restriction digestion of pGEM-T Easy-RING constructs with *Bam* HI and *Xho* I.

Figure 3.5: 1% agarose gel electrophoresis showing restriction digestion of pGEX-6P-2-RING_sl with *Bam* HI and *Xho* I.

Figure 3.6: Coomassie Blue stained proteins separated by a 16% SDS PAGE gel electrophoresis showing small-scale screen for GST-RING_sl expression.

Figure 3.7: Large-scale expression and affinity purification of GST-RING_sl and its separation from GST by 3C protease.

Figure 3.8: Removal of residual GST from RING_sl by anion exchange chromatography.

Figure 3.9: Removal of residual GST and small molecules from purified RING_sl by size exclusion chromatography.

Figure 3.10: Removal of residual GST and small molecules from purified RING_ss by size exclusion chromatography.

Figure 3.11: Coomassie Blue stained proteins analysed using 16 % SDS PAGE gel electrophoresis showing the final concentrated RING_sl in 5 mM DTT.

Figure 3.12: The Bradford Assay standard curve obtained for quantifying the concentration of RING_sl.

Figure 3.13: Quantification of RING_sl protein concentration by NanoDrop spectrometry.

Chapter 4

Figure 4.1: 1D spectrums of RING constructs, pH6.0, 25°C, recorded at 600 MHz.

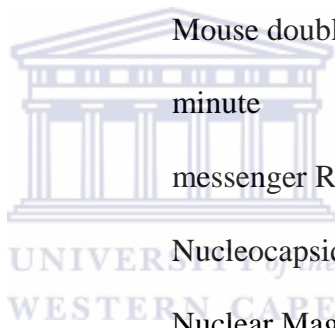
- Figure 4.2: ^{15}N -HSQC spectrums of RING constructs, pH 6.0, 25°C, recorded at 600 MHz
- Figure 4.3: Overlay ^{15}N -HSQC spectra of RING_sl (black) domain and previous RING full (red), pH6.0, 25°C, recorded at 600 MHz.
- Figure 4.4: Determination of the molecular mass of RING_sl using mass spectrometer.
- Figure 4.5: 1D spectra of RING_sl, at different pH conditions.
- Figure 4.6: Superimposition of ^{15}N -HSQC spectra of RING_sl, pH 6.0, 25 °C, recorded at 600 MHz, before (black) and 2 weeks after (red) the addition of 2 mM ^{113}Cd -EDTA.
- Figure 4.7: Separation of the unfolded/aggregated protein from the folded protein and the removal of excess Cadmium/Zinc to determine the stability of Cadmium/Zinc in RING_sl using size exclusion chromatography.
- Figure 4.8: ^{15}N -HSQC spectra of RING_sl, pH 6.0, 25 °C, recorded at 600 MHz, showing the removal of excess cadmium/zinc, and aggregated protein using size exclusion chromatography.
- Figure 4.9: Cadmium/zinc exchange experiments monitored by 1D directly detected and correlation experiments.
- Figure 4.10: ^{113}Cd -HSQC spectrum of the cadmium-exchanged RING_sl sample.

Abbreviations

Å	Angstrom
AIRE1	Autoimmune regulator protein
APS	Ammonium persulphate
Asp,D	Aspartic acid
ATP	adenosine tri-phosphate
ATR	Attenuated total reflection
bp	base pair
Brca1	Breast cancer 1 gene
BSA	Bovine Serum Albumin
C-terminus	Carboxyl terminus
CAF1	CCR4-associated factor 1/POP2
CCR4	carbon catabolite repressor 4
CD	Circular Dichroism
^{113}Cd , Cd^{2+}	Cadmium ion
Co^{2+}	Cobalt ion
CV	Column volume
Cys,C	Cysteine
Cyt <i>c</i>	Cytochrome <i>c</i>
DNA	Deoxyribonucleic acid
dNTP	2'-deoxynucleoside 5'-triphosphate

DRIL	Double RING finger linked
DTT	1,4-dithio-DL-threitol
E1s	E1 ubiquitin-activating enzyme
E2s	E2 ubiquitin conjugating enzyme/Ubc
E3s	E3 ubiquitin ligase.
EDTA	Ethylenediaminetetra acetic acid
FTIR	Fourier Transform Infrared spectroscopy
Fig	Figure
Gln,Q	Glutamine
Glu,E	Glutamic acid
Gly,G	Glycine
GST	Glutathione S-Transferase
HDM2	Human double minute 2
HHARI	Human homologous of <i>Drosophila</i> Ariadne
HECT	Homologous to the E6-AP Carboxyl
His,H	Histidine
HSQC	Heteronuclear Single Quantum Coherence Spectroscopy
Ile,I	Isoleucine
IBR	In Between RING
ICS-OES	Inductively coupled plasma optical emission
IEEVH	Equine Herpes Virus Protein
IPTG	Isopropyl-1-thio -D-galactoside

IR	Infrared Radiation
Kb	kilo base
kDa	kilo Dalton
Leu,L	Leucine
LB	Luria broth
LIM	Lin11/Isl-1/Mec-3
Lys, K	Lysine
MAT1	Ménage à trios
MBP	Maltose binding protein
MDM2	Mouse double minute 2
min	minute
mRNA	messenger RNA
Ncp7	Nucleocapsid protein
NMR	Nuclear Magnetic Resonance
NOESY	Nuclear Overhauser Enhancement Spectroscopy
N-terminus	Amino terminal
P2P-R	proliferation potential protein-related
PACT	p53-Associated Cellular protein-Testes derived
PAGE	Polyacrylamide gel electrophoresis
PBS	Phosphate buffer saline
PCR	Polymerase Chain Reaction



PDB	Protein Data Bank
PHD	Plant homeodomain
Phe,F	Phenylalanine
ppm	parts per million
RAG1	Recombinant-activating gene 1
pRb	Retinoblastoma gene product
RBBP6	Retinoblastoma binding protein 6
RBQ-1	RB-binding Q-protein
RING	Really interesting new gene
RING_sl	RING_short-long
RING_ss	RING_short-short
RNA	Ribonucleic acid
s	seconds
Ser, S	Serine
SDS	Sodium dodecyl sulphate
SR	Serine Rich
TBE	Tris Borate EDTA
TE	Tris EDTA
TFIIH	Transcription factor IIH
Thr,T	Threonine
TPEN	N,N,N',N'-tetrakis (2-pyridylmethyl)
Trp, W	Tryptophan
Ubc	Ubiquitin conjugating enzymes



UV

Ultra Violet

Zn²⁺

Zinc ion



Table of contents

Title	i
Keywords	ii
Abstract	iii
Declaration	v
Dedication	vi
Acknowledgements	vii
List of tables and figures	viii
Abbreviations	xii
Chapter 1: General Introduction	1
1.1 Introduction	1
1.2 Retinoblastoma binding protein 6 (RBBP6)	2
1.3 RING finger domains	4
1.3.1 C3HC4, C3HHC3, C4C4 and C2H2C4 RING finger domains	4
1.3.2 PHD (Plant homeodomain)	6
1.3.3 U box domain	6
1.4 Functions of RING finger domains	7
1.4.1 Ubiquitination	7
1.4.2 Other functions of RING fingers	9



1.5	Chemistry of zinc coordination	10
1.6	The use of heteronuclear NMR to investigate Zn ²⁺ binding in RING fingers	11
1.7	The use of ¹¹³ Cd exchange experiments to study Zn ²⁺ coordination by RING finger domains	12
1.7.1	Replacement of Zn ²⁺ by Cd ²⁺ in the p44 RING domain	13
1.7.2	Replacement of zinc by cadmium in the CNOT4 RING domain	15
1.7.3	Binding sites of Zn ²⁺ and Cd ²⁺ in cytochrome c	16
1.7.4	Kinetics of metal exchange and Binding affinities	17
1.8	Aims of the study	18

CHAPTER 2: Materials and methods

2.1	Stock solutions buffers and bacterial strains	19
2.2	Generation of DNA expression constructs	22
2.2.1	Primer design	22
2.2.2	PCR amplification	23
2.2.3	Colony PCR assays	23
2.2.4	Cloning of PCR products and restriction fragments	24
2.2.5	Restriction digestion	26
2.2.6	DNA Sequencing	26
2.2.7	Plasmid DNA isolation	27
2.2.8	Transformation of plasmid DNA into competent cells	28

2.3	Expression and affinity purification of recombinant protein	28
2.3.1	Small-scale protein expression screen	28
2.3.2	Large-scale expression of recombinant protein	29
2.3.3	Glutathione-affinity purification of GST fusion proteins	30
2.3.4	Cleavage of GST fusion proteins using 3C protease	30
2.3.5	Anion exchange chromatography	31
2.3.6	Size exclusion chromatography	31
2.4	Agarose gel electrophoresis of DNA	32
2.5	SDS-PAGE gel electrophoresis	32
2.6	Bradford Assay	33
2.7	NMR analysis and characterisation of zinc binding	34
2.7.1	Sample preparation	34
2.7.2	NMR data collection and processing	34
2.7.3	Replacement of Zn ²⁺ by ¹¹³ Cd	34
2.7.4	pH sensitivity measurements	35
2.7.5	Prediction of protein parameters	35

Chapter 3: Recombinant expression and purification of shortened RING finger domains 36

3.1	Cloning of shortened RING constructs into the pGEX-6P-2 expression vector	37
3.1.1	PCR amplification of RING finger domains	37

3.1.2	Cloning of RING fragments into the pGEM-T Easy vector	37
3.1.3	DNA sequencing	38
3.2	Expression and affinity purification of GST-RING_sl and GST-RING_ss	39
3.3	Cleavage of GST-RING_sl and GST-RING_ss and removal of GST by affinity chromatography	39
3.4	Final purification of RING_sl and RING_ss	40
3.4.1	Anion exchange chromatography	40
3.4.2	Size exclusion chromatography	40
3.5	Determination of protein concentration	41
3.6	Calculation of the molar extinction coefficient	42
Chapter 4: NMR analysis of zinc coordination by the RBBP6 RING domain		44
4.1	Preliminary NMR analysis	44
4.2	Investigation of Zn ²⁺ binding using mass spectrometry	45
4.3	Investigation of Zn ²⁺ binding using NMR	46
4.3.1	pH sensitivity measurement	47
4.3.2	Perturbation of ¹⁵ N-HSQC spectra	47
4.3.3	Refolding induced by Zn ²⁺ and Cd ²⁺	48
4.3.4	Direct detected ¹¹³ Cd NMR experiments	49
4.3.5	¹¹³ Cd- ¹ H coherence transfer experiments	49
Chapter 5: Discussion and conclusion		51

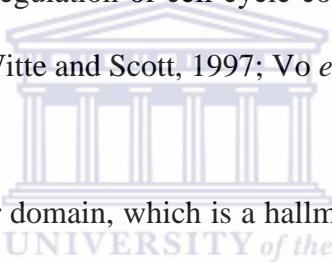
References	54
Appendix I: Amino acid sequence of the original RBBP6 RING and the shortened constructs	58
Appendix II: Sequence analysis of RING_sl cloned into pGEM-T Easy	59
Appendix III: Sequence analysis of RING_ss cloned into pGEX-6P2 expression vector	61
Appendix IV: Prediction of protein parameters	63



Chapter 1: General Introduction

1.1 Introduction

Retinoblastoma binding protein 6 (RBBP6) is a 250 kD human protein that is known to interact with tumour suppressor proteins p53 and retinoblastoma (pRb) (Sakai *et al.*, 1995; Simons *et al.*, 1997) and to be essential for the ubiquitination of p53 by Hdm2 (Li *et al.*, 2007). RBBP6 is highly expressed in oesophageal cancer cells and has been shown to be a promising target for immunotherapy against the disease (Yoshitake *et al.*, 2004). In addition to its interaction with p53 and pRb, RBBP6 is also known to be involved in a variety of functions including regulation of cell cycle control, apoptosis and pre-mRNA splicing (Simons *et al.*, 1997; Witte and Scott, 1997; Vo *et al.*, 2001).

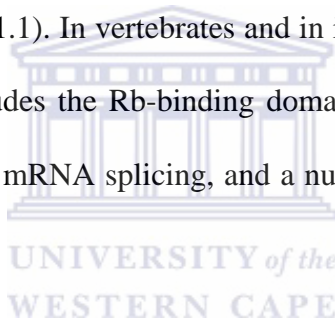


RBBP6 contains a RING finger domain, which is a hallmark of E3 ubiquitin ligases, and which is essential for the interaction with Hdm2 (Li *et al.*, 2007). RING fingers typically bind two Zn^{2+} ions, coordinated by eight conserved cysteine or histidine residues, typically forming a C3HC4 motif, although a number of other possibilities including C4C4 and C4HC3 have been reported. Sequence alignments suggest that the RBBP6 RING is either a C4C4 or possibly a novel C3NC4 RING. Sequence alignments show furthermore that RBBP6 could also be classified as a member of the U box family, which do not bind Zn^{2+} , and in which the Zn^{2+} coordinating bonds are replaced by hydrophobic interactions. However they adopt the same structures as RING fingers. The aim of this work was to use NMR to investigate the Zn^{2+} binding characteristics of the RBBP6 RING finger domain in order to establish whether Zn^{2+} was required for folding, and whether

Zn²⁺ could be replaced by Cd²⁺, as had been done successfully in a few other proteins, if possible, to establish the identities of the residues involved in coordinating the Zn²⁺ ions.

1.2 Retinoblastoma binding protein 6 (RBBP6)

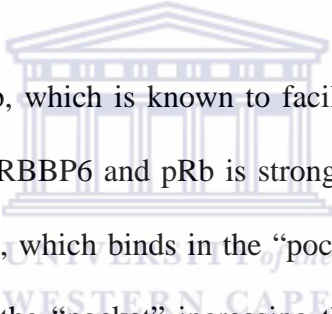
RBBP6, also known as PACT (p53-Associated Cellular protein-Testes derived), P2P-R (Proliferation Potential protein-Related) or RBQ-1 (RB-binding Q-protein) is a 250 kD protein that interacts with tumour suppressor proteins p53 and pRb (Sakai *et al.*, 1995; Simons *et al.*, 1997; Gao *et al.*, 2002). A shorter three-domain form of the protein, consisting of the DWNN domain, a Zinc finger and a RING finger domain, is found in all eukaryotic organisms (see Fig 1.1). In vertebrates and in insects the protein has a long C-terminal extension which includes the Rb-binding domain, p53-binding domain, an SR region known to play a role in mRNA splicing, and a nuclear localisation domain (Pugh *et al.*, 2006).



Similar to other SR domain-containing proteins, RBBP6 localises to nuclear speckles and associates with Sm antigens in nuclear extracts, suggesting a role for RBBP6 in mRNA splicing (Simons *et al.*, 1997). Mpe1p, which is the yeast homologue of RBBP6, is an essential protein, which forms part of the yeast cleavage and polyadenylation complex. Neutralisation of Mpe1p by the addition of anti-Mpe1p antibodies completely inhibited polyadenylation of mRNA transcripts (Vo *et al.*, 2001).

The interaction of RBBP6 and p53 can strongly interfere with the binding of p53 to DNA (Simons *et al.*, 1997). RBBP6 has been shown to reduce the transcriptional activity of

p53. Removal of RBBP6 using RNAi in cells resulted in the accumulation of p53, leading to inhibition of growth followed eventually by cell death, suggesting that RBBP6 is anti-apoptotic (Li *et al.*, 2007). Conversely Gao and Scott showed that over-expression of RBBP6 in cells promotes cell cycle arrest and mitotic apoptosis (Gao and Scott, 2002). Although these results would appear to be contradictory, together they suggest that RBBP6 plays an important poorly understood role in the regulation of p53 and hence, in the control of cancer. In support of this hypothesis RBBP6 has been shown to be highly expressed in oesophageal cancer and to be a promising target for immunotherapy against this form of cancer (Yoshitake *et al.*, 2004).

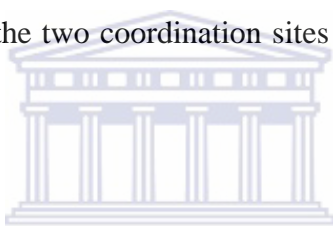


RBBP6 also interacts with pRb, which is known to facilitate terminal differentiation in cells. The interaction between RBBP6 and pRb is strongly inhibited by adenovirus E1a protein (Witte and Scott, 1997), which binds in the “pocket”, region of pRb, suggesting that RBBP6 may also bind in the “pocket” increasing the likelihood of the interaction playing a biological role.

The presence of a RING finger domain and a ubiquitin-like domain has led to RBBP6 being identified as an E3 ubiquitin ligase (Pugh *et al.*, 2006). Li *et al.*, recently reported that RBBP6 is required for ubiquitination of p53 via Hdm2 the human analogue of Mdm2 protein (Li *et al.*, 2007). This suggests a possibility for the RBBP6 RING finger domain to act as an E3 ubiquitin enzyme.

1.3 RING finger domains

A RING finger is a cysteine rich domain containing a $CX_2CX_{9-39}CX_{1-3}HX_{2-3}(C/H)X_2CX_{4-48}CX_2C$ consensus sequence (Joazeiro and Weissman, 2000; Capili *et al.*, 2004), where X can be any amino acid (see Fig 1.2). Eight cysteine or histidine residues coordinate two Zn^{2+} ions in a cross-brace manner, in which the first and third Cys/His pairs coordinate the first Zn^{2+} ion and the second and fourth pairs coordinate the second Zn^{2+} ion (see Fig 1.3). The spacing observed between the second and third Zn^{2+} coordinating pair is a unique character that is conserved amongst all RING finger domains, corresponding to the physical distance between the two coordination sites (Hanzawa *et al.*, 2001; Pickart, 2001; Capili *et al.*, 2004).



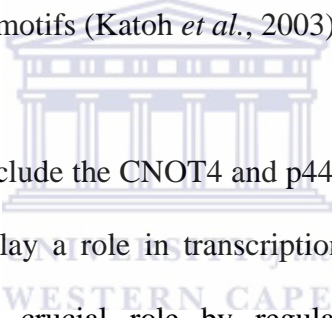
The overall secondary structure of the RING finger domain consists of a single three-stranded anti-parallel β -sheet and an α -helix, connected by long loops, as shown in Fig 1.4 (Kellenberger *et al.*, 2005). The ability of the ~70 amino acid residue RING finger domain to fold independently is due to its ability to coordinate two Zn^{2+} ions, which stabilize the structure (Pickart, 2001).

1.3.1 C3HC4, C3HHC3, C4C4 and C2H2C4 RING finger domains

The initial consensus sequence for coordinating Zn^{2+} ions by RING finger motifs was defined as C3HC4 (Krishna *et al.*, 2003), in which the first Zn^{2+} ion is coordinated by three cysteine residues and a histidine residue while the second Zn^{2+} ion is coordinated by four cysteine residues. Examples of the C3HC4 motif include the RAG1, MAT1, c-

Cbl, IEEVH and BRCA1 proteins. The definition of the consensus sequence has recently expanded to include sequences such as C3HHC3, the C4C4, and the C2H2C4 motif.

An example of the C3HHC3, which is also known as RING-H2, is provided by the EL5 RING-H2 (Katoh *et al.*, 2003). In this motif Cys 4 is replaced by a His residue. EL5 is related to proteins of the *Arabidopsis* ALT family and includes a transmembrane domain, a basic domain, a conserved domain and the RING-H2, which are named domain I-IV respectively. The long C-terminal domain is poorly conserved (see Fig 1.8a). The structure of the RING-H2 presents a $\beta\beta\alpha$ fold with large N- and C-terminal loops, which is similar to other RING finger motifs (Katoh *et al.*, 2003).

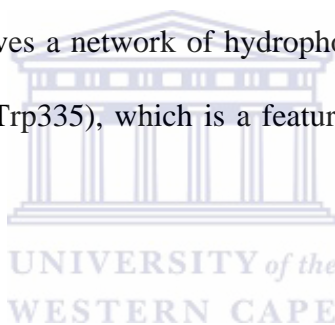


Examples of the C4C4 motif include the CNOT4 and p44 RING finger domains (Houben *et al.*, 2005), both of which play a role in transcriptional regulation. Hdm2 is an E3 ubiquitin ligase that plays a crucial role by regulating the amount of p53 via ubiquitination. It encodes a C2H2C4 motif at its C-terminal region, which coordinates two Zn^{2+} ions, and has recently been shown to adopt the same $\beta\beta\alpha\beta$ fold as other RING fingers (Kostic *et al.*, 2006).

Fig 1.2 shows an alignment of RBPP6 RING finger against a number of RING motifs. The histidine (H) at position 4 has been replaced by an asparagine (N), and an extra cysteine (C) has been inserted immediately adjacent to the cysteine at position 3. Hence is not yet clear whether the RBPP6 RING finger should be described as a C4C4 or as a C3NC4 RING finger motif.

1.3.2 PHD (Plant homeodomain) RING-like domain

Plant homeodomain (PHD) finger domains are structurally related to RING finger domains and can be characterized as a C4HC3 motif (Dul and Walworth, 2007). The conserved ~60 residue PHD finger domain occurs in over 400 eukaryotic proteins, many of which are involved in the regulation of gene transcription. The 3D NMR structure of the PHD of the Autoimmune regulator protein (AIRE1) is shown in Fig 1.5. The PHD adopts a $\beta\beta\alpha\beta$ topology similar to classical RING finger or U box domains (Bottomley *et al.*, 2005), although the α -helix forms part of the second Zn^{2+} ion coordination site rather than the first (see Fig 1.3). In addition to Zn^{2+} coordination, stabilisation of the PHD finger domain also involves a network of hydrophobic residues, which surround a highly conserved tryptophan (Trp335), which is a feature common to all PHD domains (Bottomley *et al.*, 2005).



1.3.2 U box domain

Zn^{2+} coordination by RING fingers is important for folding and stability, but it is not required in domains such as the U box, which lacks the metal coordinating residues. The U box motif was first identified in the yeast protein UFD2 (ubiquitin fusion degradation protein 2) and subsequently shown to be present in other eukaryotic proteins (Pringa *et al.*, 2001). Although the U box lacks the Zn^{2+} coordinating residues, it adopts the same topology and 3D structure as RING fingers (Houben *et al.*, 2005).

In the U box domain the Zn^{2+} coordinating residues are replaced by a set of hydrophobic residues (see Fig 1.2) interconnected by salt bridges and hydrogen bonds, which stabilize

the U box domain (Andersen *et al.*, 2004). Many of these residues are also conserved in the RING finger domains, however the degree of conservation is higher in the U box domains. For example, the RBBP6 RING finger domain can also be classified as a U box domain due to the conservation of the hydrophobic residues also found in the U box domain (Aravind and Koonin, 2000). However the presence of conserved cysteines, in addition to the hydrophobic residues, suggests that the RBBP6 domain does bind Zn^{2+} ions and is therefore a RING finger rather than a U box domain. U box domains, like RING fingers, act as E3 ubiquitin ligases and mediate ubiquitination in the same way as the RING finger domains (Aravind and Koonin, 2000).

1.4 Functions of RING finger domains

RING finger domains form a large group of Zn^{2+} coordinating proteins with wide range of functions (Pickart, 2001), which include ubiquitination, cell growth, differentiation and multimerization.

1.4.1 Ubiquitination

RING finger-containing proteins act as E3 ubiquitin ligases during ubiquitination. Ubiquitination refers to post-translation modification of proteins by covalent attachment of one or more ubiquitin monomers. Ubiquitination acts as a signal, activating a number of important pathways, including degradation of the ubiquitinated protein by the 26S proteasome, quality control, vesicular trafficking, receptor endocytosis, transcriptional regulation and DNA repair. Since proteins are continuously synthesized in the cell they must also be degraded. Degradation is essential to the cell in order to supply amino acids

for new protein synthesis and to remove excess enzymes and transcriptional factors that are no longer needed or proteins that have been damaged.

Ubiquitination is mediated by several enzymes, namely: (1) an E1 ubiquitin-activating enzyme, an E2 ubiquitin-conjugating enzyme/Ubc and (3) an E3 ubiquitin ligase. During ubiquitination the E1 enzyme activates ubiquitin in an ATP-dependant manner, forming a thiol-ester bond between the E1's catalytic cysteine and ubiquitin's C-terminus. The E1 enzyme then transfers ubiquitin to the catalytic cysteine of the E2 enzyme (Zolk *et al.*, 2006). E3 ubiquitin ligases play a role in substrate recognition, during the transfer of ubiquitin to the E3 ubiquitin ligase (Fig 1.6), and bind both the E2 and the target. E3 ubiquitin ligase transfers the activated ubiquitin from the E2 enzyme to the ϵ -amino group of a lysine on the target protein, thereby forming an iso-peptide bond. E3 ubiquitin ligases therefore play a crucial role in recognizing and selecting the protein that is to be degraded (Pringa *et al.*, 2001; Zolk *et al.*, 2006). Like other RING fingers containing proteins, RBBP6 mediates ubiquitination of p53 via its interaction with Hdm2 (Li *et al.*, 2007).

E3 ubiquitin enzymes are classified into two main groups: those containing a HECT (Homologous to the E6-AP Carboxyl Terminus) domain and the larger group of those containing a RING finger domain, or the closely related U box domain (Pickart, 2001). The HECT domain is made up of ~350 residues (Pickart, 2001). It catalyzes the ubiquitination reaction by forming a Ub-thioester intermediate between ubiquitin and a

conserved cysteine residue in the HECT domain (Kumar *et al.*, 1997; Huang *et al.*, 1999; Joazeiro and Weissman, 2000).

A family of HECT domain proteins called the WW domains recognizes a specific sequence PPxY (PY motif) and other proline-rich motifs. The WW domains include proteins with a variety of functions including Nedd4 and E6-AP. Nedd4 mediates the ubiquitination and downregulation of an epithelial cell sodium channel (maintains electrolyte homeostasis), whereas the E6-AP mediates ubiquitination and degradation of p53 protein induced by papillomavirus (Huang *et al.*, 2000).

1.4.2 Other functions of RING fingers

RING finger-containing proteins play vital roles in cell growth, differentiation and multimerization (Kato *et al.*, 2003). Li *et al.*, showed that knocking down RBBP6 in mice leads to early embryonic lethality, suggesting that RBBP6 is important for cell growth and embryonic development (Li *et al.*, 2007). Recombinant-activating gene 1 (RAG1) plays a role in the recombination of immunoglobulin and the T cell receptor genes. RAG1 encodes a highly conserved C3HC4 RING finger at its N-terminal region, as well as C2H2 Zn²⁺ finger motifs at its N and C-terminal ends respectively. One of the C2H2 Zn²⁺ finger motifs forms a dimer with C3HC4 RING finger, suggesting that the RING domain is involved in protein-protein interactions (Rodgers *et al.*, 1996; Yurchenko *et al.*, 2003).

1.5 Chemistry of Zn²⁺ coordination

Zn²⁺ coordination is important for folding, structural stability and functional activity of metalloproteins (Houben *et al.*, 2005). Transcription factors and other enzymes require Zn²⁺ for their function. Zn²⁺ binding proteins are classified as those in which Zn²⁺ ions serve either a catalytic or structural purpose. The focus of this review is on Zn²⁺ binding proteins, which Zn²⁺ serves a structural purpose. Examples of Zn²⁺ binding proteins include C2H2, C3H and C4 Zn²⁺ fingers and RING fingers. Zn²⁺, unlike other divalent ions, is ligated by ligands such as Cys and His residues, although it can also be found coordinated by side chains of Asp or Glu (Dudev and Lim, 2003). Zn²⁺ adopts a tetrahedrally, pentahedral or octahedral coordination, depending on the protein and the solvent accessibility of the metal binding site. The presence of more than one His, Asp or Glu side chains increases the chances of a tetrahedral coordination over octahedral/pentahedral coordination, regardless of the nature of the metal binding site. However tetrahedral coordination is the most stable and is known to occur in all structural Zn²⁺ binding sites in proteins (see Fig 1.7). Zn²⁺ favours tetrahedral coordination because it is buried away from the solvent, and because polarizable Cys side chains transfer more charge than water, neutralising the positive charges on Zn²⁺ (Dudev and Lim, 2003).

Zn²⁺ binding sites in proteins are also accessible to heavy metals like Cd, Hg and Pb. The C4 protein motifs bind Cd ion and Pb ion more tightly than Zn²⁺ ion, whereas the C2H2 and C2HC protein motif bind Zn ion more tightly. The larger radius of Cd²⁺ (0.95 Å) compared to (0.75 Å) for Zn²⁺ results in Cd-N bonds (His) and Cd-S (Cys) of 2.1-2.3 Å

and 2.6 Å respectively, compared to 2.1 Å and 2.3 Å for Zn-N (His) and Zn-S (Cys) (Dudev and Lim, 2003).

1.6 The use of heteronuclear NMR to investigate Zn²⁺ binding in RING fingers.

Heteronuclear NMR spectroscopy has been used successfully to demonstrate the requirement of Zn²⁺ ions for folding of RING finger domains as well as to directly identify the residues responsible for coordinating the two Zn²⁺ ions (Hanzawa *et al.*, 2001; Katoh *et al.*, 2003; Capili *et al.*, 2004). The ¹⁵N-HSQC spectrum of a protein is a 2-dimensional spectrum in which each resonance corresponds to one backbone NH group, with the horizontal coordinate corresponding to the chemical shift of the proton and the vertical coordinate corresponding to the chemical shift of the attached nitrogen (see Fig 1.8b). Exceptions are the pairs of peaks corresponding to side chain NH₂ groups of asparagine and glutamine residues, which can be found at the right hand corner of the spectrum. Proline residues do not appear in the ¹⁵N-HSQC spectrum, because they lack backbone NH groups. In order to be observable the N nuclei need to be ¹⁵N isotopes rather than the more common ¹⁴N, which is accomplished by expressing the protein sample in bacteria grown on media in which the only source of nitrogen is ¹⁵N-enriched ammonium chloride (Rehm *et al.*, 2002).

The dispersion of the resonances in the ¹⁵N-HSQC of a folded protein is significantly greater than for an unfolded protein, making the ¹⁵N-HSQC spectrum an effective probe of protein folding, and consequently an effective indicator of the requirement of proteins to bind Zn²⁺. Using this method it was demonstrated that the addition of EDTA caused

unfolding of the RING finger from EL5 (see Fig 1.8c). Addition of EDTA resulted in the loss of a number of resonances whereas addition of Zn^{2+} restored the spectrum to its original state (Fig 1.8d). This suggests that coordination of Zn^{2+} ions by EL5 RING-H2 is essential for folding and structural stability (Kato *et al.*, 2003).

Human homologous of *Drosophila* Ariadne (HHARI) is a protein containing two RING finger domains (RING1 and RING2) separated by a cysteine rich domain called an “In Between RING” domain (see Fig 1.9a). RING2 adopts a 3D fold, which is different from classical RING fingers because His4 and Cys8 in classical RING finger motif are not conserved. As confirmed by mutational studies and Zn titration experiments, ICP-OES (Inductively coupled plasma optical emission spectroscopy) measurements demonstrated that there is 1:1.3 ratio of RING2 to Zn^{2+} content, which suggests that RING2 coordinate only one Zn^{2+} ion. The requirement for Zn^{2+} for folding of RING2 was also investigated using ^{15}N -HSQC NMR spectra. The spectrum in Fig 1.9 shows that RING2 is folded when expressed in the presence of Zn^{2+} , but unfolded when expressed in the absence of Zn^{2+} (Capili *et al.*, 2004).

1.7 The use of ^{113}Cd exchange experiments to study Zn^{2+} coordination by RING finger domains

NMR can be used to investigate Zn^{2+} coordination by replacement by Cd^{2+} ions. The identities of the residues involved in coordinating the two Zn^{2+} ions is typically inferred from (1) the pattern of conservation of Cys and His residues, which are known to be capable of forming coordination bonds with Zn^{2+} ions, and (2) the proximity of the

conserved residues to the Zn^{2+} ions in solved structure. NMR provides a method of directly identifying the amino acids coordinating the metal ion, by transfer of magnetic energy from the metal ion to protons within the coordinating amino acid.

In the case of cysteine the closest protons to the metal ion are the H^β protons, which are separated from the metal ion by three covalent bonds plus the coordination bond (see Fig 1.10). Magnetisation transfer between the metal ion and the H^β proton can be observed using an HSQC spectrum similar to the one described in Section 1.6. However since Zn^{2+} nuclei have no NMR signal, another metal ion such as $^{113}Cd^{2+}$, which does have an NMR signal and has similar chemical properties to Zn^{2+} , must be used. It has previously been shown that Cd^{2+} can replace Zn^{2+} in proteins without significant disruption of the folded structure. Cd^{2+} is the most compatible ion to replace Zn^{2+} because its radius is only marginally larger than that of Zn^{2+} (0.99 Å as compared to 0.74 Å) (Hanzawa *et al.*, 2001). Although not large enough to disrupt the folded structure the increase in size is sufficient to perturb the ^{15}N -HSQC spectrum of the protein. Exchange of Zn^{2+} by Cd^{2+} typically leads to the disappearance of resonances close to the coordination site accompanied by the appearance of resonances corresponding to the Cd^{2+} -bound form of the protein (Hanzawa *et al.*, 2001; Houben *et al.*, 2005).

1.7.1 Replacement of Zn^{2+} by Cd^{2+} in the p44 RING domain

The DNA (TFIIH) transcriptional factor IIH p44 plays a central role in the transcription activities of TFIIH. Mass spectrometry showed that the C-terminal C4C4 RING domain of p44 coordinates two Zn^{2+} ions (Houben *et al.*, 2005; Kellenberger *et al.*, 2005). The

structure of the domain resembles that of classical RING fingers, although the last β -strand (β 3), which is located at the C-terminus of C3HC4 RING fingers, is located at the N-terminus of the p44 domain.

Zn^{2+} binding in p44 was investigated using NMR, following addition of ^{113}Cd -EDTA to a Zn^{2+} -containing p44 protein sample to a final concentration of 4 mM. Exchange of Zn^{2+} by Cd^{2+} was completed within 6 hours, as monitored by the disappearance of some peaks and the appearance of new peaks on the ^{15}N -HSQC spectrum, which show exchange between the Zn^{2+} -bound and Cd^{2+} -bound forms. Only a small number of resonances were affected, indicating that the exchange did not affect the integrity of the structure as a whole (see Fig 1.11A). The chemical shift differences (Fig 1.11A) were observed for four different regions: Cys345-Cys348, Cys360-Cys363, Cys368-Cys371 and Cys382-Cys385. The exchange caused large chemical shifts perturbations for residues Gly347, Val362, Cys363, Cys371, Gly384, Cys385 and His387, which are most probably due to the breaking of hydrogen bonds between the amide protons of these residues and the sulfur atoms of the preceding cysteine residues.

The ^{113}Cd -HSQC spectrum in Fig 1.11B shows the coherence transfer between the H^{β} protons of the coordinating cysteine residues and the bound ^{113}Cd ions. The ^{113}Cd chemical shifts in Fig 1.11B are reported relative to $CdSO_4$. The ^{113}Cd -HSQC spectrum consists of two horizontal lines of peaks, indicating that there are two chemically distinct Cd^{2+} ions present in the samples, with chemical shifts of 676.5 ppm and 695.0 ppm respectively. The coordinating protons have chemical shifts in the range 2.5-4.0 ppm,

which are characteristics of Cys H^β protons. From knowledge of the chemical shifts assignments of the Cys resonances, it was deduced that the Cd at 695.0 ppm coordinates Cys 345,348,368 and 371, and therefore is identified as Cd I, while the Cd at 676.5 ppm coordinates Cys 360, 363, 382, and 385 and is identified as Cd II, indicating that Cd²⁺/Zn²⁺ ions are coordinated in a cross-brace manner (Kellenberger *et al.*, 2005).

1.7.2 Replacement of Zn²⁺ by Cd²⁺ in the CNOT4 RING domain

NOT4 is human protein forming part of the CCR-NOT complex, which plays a role in transcriptional regulation by interacting with RNA polymerase II. Its N-terminal region contains a C4C4 RING finger, with a Cys-X₂-Cys-X₁₃-Cys-X-Cys-X₄-Cys-X₂-Cys-X₍₁₁₋₁₆₎-Cys-X₂-Cys motif (Hanzawa *et al.*, 2001; Albert *et al.*, 2002). Although the CCR4-NOT4 coordinates Zn²⁺ ions using a C4C4 motif, and the spacing observed between the fourth and the fifth coordinating residues is different from other C3HC4 RING fingers, (X₄ rather X_{2,3}), it nevertheless adopts the same topology (Hanzawa *et al.*, 2001).

Exchange of Zn²⁺ by Cd²⁺ was achieved by adding ¹¹³Cd-EDTA to a final concentration of 4 mM and monitored by ¹⁵N-HSQC spectra. Assignment of the Cd²⁺-bound species was confirmed by 3D NOESY- (¹H,¹⁵N)-HSQC and 3D TOCSY-(¹H, ¹⁵N)-HSQC spectra. Large chemical shift differences were found for Cys17, Cys33 and Cys56 for both ¹H and ¹⁵N chemical shifts (see Fig 1.12A). Other residues experienced smaller chemical shift changes, indicating that the exchange had no effect on the integrity of the whole structure (Hanzawa *et al.*, 2001).

Zn²⁺ coordination was investigated using ¹¹³Cd-HSQC spectrum. As for the CNOT4 RING finger, two chemically distinct Cd²⁺ resonances are observed with chemical shifts of 687.5 and 714.4 ppm respectively. The Cd at 687.5 ppm is coordinated to Cys14, 17, 38 and 41, and the Cd at 714.4 ppm is coordinated to Cys33, 53, and 56 (see Fig 1.12B). Although the correlation of Cys31 with the Cd was not directly observed in the ¹¹³Cd-HSQC spectrum it was taken to be the fourth residue coordinating Cd II on the basis of its conservation. With only this assumption the observed pattern agrees with the cross-brace pattern observed for C3HC4 RING fingers (Hanzawa *et al.*, 2001).

1.7.3 Binding sites of Zn²⁺ and Cd²⁺ in cytochrome c

Cytochrome *c* is one of a number proteins associated with the mitochondrial membrane, which mediate electron shuffling between ubiquinol-cytochrome *c* oxidoreductase and cytochrome *c* oxidase during respiration. Loss of Cytochrome *c* from the mitochondrial membrane leads to apoptosis. Binding of Zn²⁺ or Cd²⁺ is known to slow down the oxidative kinetics of Cytochrome *c* as monitored by H₂O₂ production. NMR was also used to monitor the binding of Zn²⁺ or Cd²⁺ ions (Gourion-Arsiquaud *et al.*, 2005).

Fig 1.13 shows the ¹⁵N-HSQC spectra obtained before (red) and after (black) the addition of Zn Acetate to the protein. Chemical shift changes induced by the exchange are shown in circles. Zn²⁺ binding residues include His33, Glu104, Ala103, Thr102, and Lys99. Glu104 experienced the largest shift, from which it was concluded that it is the major residue involved in Zn²⁺ coordination. (Gourion-Arsiquaud *et al.*, 2005).

1.7.4 Kinetics of metal exchange and binding affinities

RING finger domains coordinate two Zn^{2+} ions, but the strength with which the two ions are coordinated differs. The C3HC4 RING finger domains of LIM, BRCA1 and Hdm2 all show differences in the affinities of the two sites. The difference can be ascribed to a number of factors including: (1) differences in the chemical environment, (2) the structure and (3) the dynamical state of the two sites (Houben *et al.*, 2005).

RING finger domains from the p44 and the CNOT4 coordinate two Zn^{2+} ions using the C4C4 motif, however the exchange rate between the two sites and between the equivalent sites in the two proteins is different. Site 1 of CNOT4 protein exchanges the metal ion twice as fast as site 2, with the opposite being true in the case of p44. Both p44 coordinating sites exchange faster than the CNOT4 sites.

The differences in the exchange rates are influenced by the chemical nature of the two coordination sites. Since Zn^{2+} and Cd^{2+} are positively charged they are exchanged faster in a negatively charged environment than in a positively charged environment. Site 2 of p44 is highly negatively charged and site 1 of CNOT4 is located close to negatively charged residues. In addition, site 2 of p44 is highly accessible to solvent, and surrounded by flexible residues which increases the likelihood of Zn^{2+} being exchanged faster than in CNOT4 (Houben *et al.*, 2005).

1.9 Aims of the study

Previous NMR analysis of a fragment of RBBP6 containing the RING finger domain have shown that the first 19 amino acids at the N-terminus are unstructured, which has hampered efforts to determine the structure of the domain. The aim of this study is to remove the unstructured residues, and then to use the shortened RING constructs to investigate the Zn^{2+} binding properties of the domain. This will be achieved by truncating the N-terminal region to produce constructs shortened by 13 and 19 amino acid residues respectively, expressed as GST-fusion proteins. After removal of the GST, 1D proton and ^{15}N -HSQC NMR spectra will be used to assess the folding and integrity of the shortened constructs, as well as the effect of lowering the pH below 6 (Zn^{2+} coordinating proteins tend to unfold in the vicinity of pH 5.5). ^{15}N -HSQC and directly detected ^{113}Cd spectra will be used to investigate whether Cd^{2+} ions can replace Zn^{2+} ions in proteins. ^{113}Cd - 1H -HSQC spectra will be used in an attempt to observe magnetic correlation transfer between the ^{113}Cd ions and protons in the side chains of the coordinating cysteine residues.

CHAPTER 2: Materials and methods

2.1 Stock solutions buffers and bacterial strains

All reagents were supplied by Promega, Bio-Rad, Merck Sigma, Roche, BDH, Invitrogen, Fermentas and Amersham Bioscience, unless otherwise stated.

Ampicillin: 100 mg/ml stock solution prepared in distilled water. Stock solution diluted 1:1000 in LB or agar media.

APS (Ammonium persulphate): 10% APS prepared by dissolving 100 mg in 1 ml distilled water and stored at 4 °C. Solution stable for up to two weeks.

5X Bradford reagent: 0.01% Coomassie Brilliant Blue G-250, 8.5% phosphoric acid, 4.75% ethanol in water.

¹¹³Cd-EDTA: 0.08 M stock solution prepared by dissolving 3.2 mg ¹¹³CdCl₂ in 27.8 µl of 0.5 M EDTA, and the volume made up to 174 µl with water.

Chloramphenicol: 34 mg/ml stock solutions prepared in 100% ethanol. Stock diluted 1:1000 in LB or agar media.

Coomassie staining solution: 250 mg Coomassie Blue R-250, 45% methanol, and 10% acetic acid.

Cleavage buffer: 0.05 M Tris-HCl, 0.15 M NaCl, 0.001 M EDTA, 0.001 M DTT, 1% Triton X 100, pH 7.0.

Destaining solution: 5% methanol, 10% acetic acid in water.

DNase I buffer: 10X stock solution prepared by dissolving 0.1 M Tris pH 7.5, 0.025 M MgCl₂, 0.005 M CaCl₂.

DNA loading buffer: 0.25% Bromophenol Blue, 0.25% xylene cyanol, 30% glycerol in distilled water.

dNTPs: 100 μ M stock solution prepared in water.

DTT (1,4-dithio-DL-threitol): 1M DTT stock solution prepared in 0.01 M sodium acetate pH 5.2, sterilized by filtration and stored at 4 °C.

GTE (Glucose Tris EDTA): 0.025 M Tris-Cl pH 8.0, 0.01 M EDTA, and 0.05 M glucose, autoclaved and stored at 4 °C.

IPTG (Isopropyl-1-thio- (D-galactoside): 0.1 M stock solution prepared by dissolving 1.19 g IPTG dissolved in 50 ml water. Solution divided into 5 ml aliquots, sterilized by filtration and stored at -20 °C. Stable for 2 to 4 months.

Luria agar: 10 g tryptone powder, 5 g yeast extract, 5 g sodium chloride, and 2 g glucose, 15 g bacteriological agar, made up to 1000 ml with distilled water and autoclaved.

Luria broth: 10 g tryptone powder, 5 g yeast extract, 5 g sodium chloride and 2 g glucose made up to 1000 ml with distilled water and autoclaved.

Lysis Buffer: 50 μ g/ml lysozyme, 35 mg/ml DNase, 1% Triton X 100, 0.001 M DTT and 1X protease inhibitor cocktail in 1X PBS.

Lysozyme: 50 mg/ml stock solution prepared in distilled water.

M9 salts: 5X salts prepared by dissolving 64 g $\text{Na}_2\text{HPO}_4 \cdot 7\text{H}_2\text{O}$, 15 g KH_2PO_4 , 2.5 g NaCl, 5.0 g NH_4Cl made up to 1000 ml with water. Solution divided into 200 ml aliquots and autoclaved.

M9 Minimal media: 200 ml 5X M9 salts, 2 ml 1 M MgSO_4 , 20 ml 20% Glucose, 0.1 ml 1 M CaCl_2 , made up to 1000 ml with autoclaved distilled water.

NaOH/SDS/ lysis solution: 0.2 N NaOH, 1% SDS.

PBS (Phosphate Buffered Saline): 10% stock solution prepared by dissolving 0.137 M NaCl, 0.0027 M KCl, 0.008 M Na₂HPO₄ and 0.0015 M KH₂PO₄ pH 7.4.

NMR buffer: 0.05 M Sodium phosphate pH 6.0, 0.15 M NaCl, 0.001 M DTT, 0.001 M EDTA and 0.02% NaA₃.

Neutralization solution: 3 M potassium acetate prepared in water. pH adjusted to 4.8 using acetic acid and stored at room temperature.

Phenol/chloroform/isoamylalcohol: 25 parts Tris saturated phenol: 24 parts chloroform and 1 part isoamyl-alcohol and stored at 4 °C.

Primers: 100 µM stock solutions stored at -20 °C.

Protein elution buffer: 0.01 M glutathione and 0.05 M Tris, pH 8.0.

RNAse (DNAse free): 100 mg/ml stock solution prepared in 0.1 M Sodium acetate and 0.0003 M EDTA pH 4.8. Solution boiled for 15 minutes and cooled quickly by placing it on ice. Stored at -20 °C.

SDS: 10% stock solution prepared by dissolving 100 g of SDS was dissolved in 900 ml water, heated to 68 °C to dissolve the crystals, and the volume made up to 1000 ml. Stored at room temperature.

2X SDS sample buffer: 4% SDS, 0.125 M Tris pH 6.8, 15% glycerol and 1 mg/ml Bromophenol Blue. Stored at room temperature. 0.2 M DTT added to the buffer immediately prior to use.

Electrophoresis buffer: 10% stock solution prepared by dissolving 30 g Tris-Cl, 144 g Glycine, 10 g SDS, made up to 1000 ml with distilled water.

Separating buffer: 1.5 M Tris pH 8.8, stored at 4 °C.

Sodium azide: 10% stock solution prepared by dissolving 10 g in 100 ml distilled water.

Stacking buffer: 0.5 M Tris pH 6.8, stored at 4 °C.

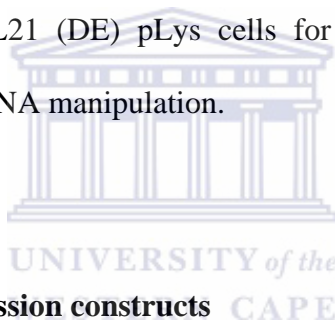
TBE: 10X stock solution prepared by dissolving 108 g Tris, 55 g boric acid, and 9.3 g EDTA, made up to 1000 ml with distilled water.

TBS-T: 17.532 g NaCl, 6.057 g Tris, 0.1% Tween 20, pH 7.5, made up to 2000 ml with distilled water.

Tris-Cl: 1 M stock solution prepared by dissolving 121.4 g in 500 ml of distilled water, pH adjusted with HCl and the volume made up to 100 ml.

TE: 10X stock solution prepared from 0.1 M Tris-Cl and 0.01 M EDTA.

Bacterial strains: *E. coli* BL21 (DE) pLys cells for protein expression and *E. coli* MC1061 competent cells for DNA manipulation.



2.2 Generation of DNA expression constructs

2.2.1 Primer design

PCR primers were designed based on the human RBBP6 gene mRNA isoform sequence (Accession number NP_008841 (protein sequence); NM_006910 (nucleotide sequence)).

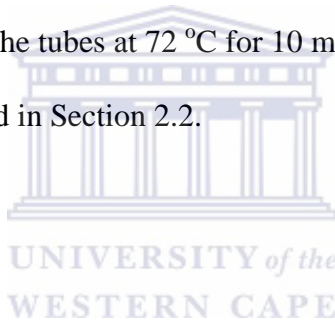
Both forward primers included *Bam* HI restriction sites while the reverse primer included an *Xho* I site for cloning into the *Bam* HI and the *Xho* I sites of the pGEX-6P-2 vector.

Two stop codons, TTA and TCA, (see Table 3.1) were included in the reverse primer.

2.2.2 PCR amplification

PCR amplifications were carried out in reactions containing 1 X PCR reaction buffer, 1 μl of 10 pM primers, 1 μl of 5 mM dNTPs, and 0.5 μl of 0.5 U/ μl Taq polymerase. 0.75 μl of 50 mM MgCl_2 was added to the reaction mixture and finally 1 μl of the template pGEX-6p-2-RING was added. The final volume was made up to 25 μl with sterile autoclaved water. The PCR tubes were briefly centrifuged and the amplification carried out under the following conditions:

94 °C for 2 mins to denature the double stranded DNA, followed by 35 cycles each consisting of the following steps: 94 °C for 1 min to denature the double stranded DNA, 62 °C for 1 min to anneal the double strands, 72 °C for 1 min to extend the DNA. The final step consisted of holding the tubes at 72 °C for 10 mins. The products were analysed on 1% agarose gels as described in Section 2.2.



2.2.3 Colony PCR assay

Colony PCR was used to screen transformed colonies for the presence of insert. Following transformation, single colonies were picked and re-suspended in 20 μl of distilled water. 1 μl of each suspension was added to the PCR reaction in place of the DNA template and the reaction carried out as described in Section 2.2.2. Where the cloning was into pGEM-T Easy vector, M13 primers with an annealing temperature of 55 °C were used; for cloning into pGEX-6P-2 vector, the primers used for the original amplification were used at an annealing temperature of 62 °C.

2.2.4 Cloning of PCR products and restriction fragments

PCR products were diluted 1:100 with sterile distilled water and cloned into the pGEM-T

Easy vector (Promega). Ligation reactions were set up as shown in Table 2.1. The ligation reactions were incubated at 4 °C for 16 hours. 10 µl of each ligation mixture was used to transform *E.coli* MC1061 competent cells, as described in Section 2.2.8. DNA restriction fragments (Section 2.1.5) were purified using the GFX kit (Amersham Bioscience: GE Healthcare, GFX PCR DNA and Gel Band purification kit) according to the manufacture's instructions and cloned into the pGEX-6P-2 expression vector. Ligation reactions were set up as shown in Table 2.2. The samples were briefly mixed and incubated at room temperature for 3 hours. 10 µl of the ligation product was used to transform BL21 and MC1061 competent cells as described in Section 2.2.8.



Table 2.1 Experimental setup for cloning PCR products into pGEM-T Easy vector

Tubes (1.5ml)	Positive control	Negative control	Experimental reaction	Reagents final concentration
pGEM-T Easy (5 ng/μl)	1 μl	1 μl	1 μl	pGEM-T Easy (0.25 ng/μl)
PCR products	0 μl	0 μl	1 μl	PCR products
Control insert (4 ng/μl)	2 μl	0 μl	0 μl	Control insert (0.4 ng/μl)
2x Rapid Ligation buffer	2 μl	2 μl	2 μl	1x Rapid Ligation buffer
T4 DNA Ligase (3 units/μl)	1 μl	1 μl	1 μl	T4 DNA Ligase (0.15 units/20 μl)
dH₂O	14μl	16 μl	15μl	
Total volume (μl)	20 μl	20 μl	20 μl	

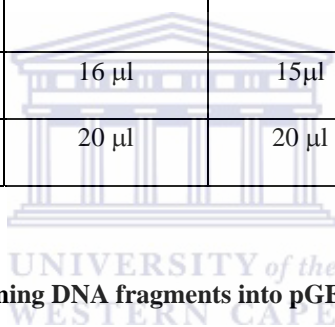


Table 2.2 Ligation reactions for cloning DNA fragments into pGEX-6P-2 expression vector

Experimental tubes with reagents	Negative control (Background)	Standard reaction
Vector (pGEX-6P-2)	1 μl	1 μl
PCR products	0 μl	3 μl
2X ligation buffer	2 μl	2 μl
T4 DNA Ligase (3 units/μl)	1 μl	1 μl
dH₂O	16 μl	13 μl
Total volume (μl)	20 μl	20 μl

2.2.5 Restriction digestion

Restriction double digests were designed using the Fermentas double digest online server ([www.fermentas.com/double digest/](http://www.fermentas.com/double-digest/)) as shown in Table 2.3. The reagents were mixed in a 1.5 ml microfuge tube and incubated at 37 °C for 1.5 hours. The samples were analysed by electrophoresis on a 1% agarose gel. The fragment corresponding to the insert was purified from the gel using the GFX kit (Amersham Bioscience: GE Healthcare, GFX PCR DNA and Gel Band purification kit) according to the manufacture’s instructions.

Table 2.3 Experimental set up for restriction double digests of pGEM-T Easy and pGEX-6P-2 vector.

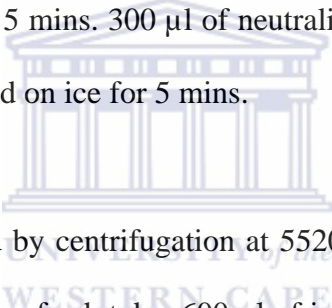
Reagents	Volume (µl)
Vector	25 µl
2X Tango™ buffer	20 µl
<i>Bam</i> HI	3 µl
<i>Xho</i> I	1 µl
dH ₂ O	1 µl
Total volume	50 µl

2.2.6 DNA Sequencing

Plates containing single colonies were sent for sequencing at Inqaba Biotechnical Industries (Pty) Ltd. Sequences were compared with the expected sequences using the Blast 2 sequence alignment tool (<http://www.ncbi.nlm.nih.gov/BLAST/bl2seq/wblast2.cgi> (Tatusova and Madden,1999)). Translations into protein sequences were carried out using the EXPASY Translate Tool (<http://au.expasy.org/tools/dna.html>). Validation of the base calling was performed by inspection of the raw sequencing trace, using the Finch TV software suite (<http://www.geospiza.com/finchtv>).

2.2.7 Plasmid DNA isolation

Small scale plasmid DNA isolation was performed using the alkaline lysis method (Birnboim and Doly, 1979). A single colony was used to inoculate 15 ml Luria-Bertani broth containing 100 µg/ml ampicillin and incubated overnight at 37 °C with shaking. From the overnight culture 900 µl was added to 100 µl of sterile glycerol for storage at -70 °C. The remaining cell suspension was centrifuged at 5520 xg for 10 min and the supernatant discarded. The pellet was re-suspended in 200 µl GTE and incubated on ice for 5 min. 400 µl lysis solution was added to the cell suspension, the mixture was mixed gently and incubated on ice for 5 mins. 300 µl of neutralising solution was added, mixed gently and the solution incubated on ice for 5 mins.



The flocculent was precipitated by centrifugation at 5520 xg for 15 mins. 800 µl of the supernatant was transferred into a fresh tube, 600 µl of isopropanol was added, mixed by vortexing and incubated at -20 °C for 1 hour. The sample was then centrifuged for 10 mins at 9.3 xg, the supernatant discarded and the pellet washed twice with 70% ethanol. The pellet was air-dried and re-suspended in 50 µl of 1X TE. 5 µl of 10 mg/ml RNase A was added and the sample incubated at 37 °C for 1 hour. Equal volume of 25 parts phenol: 24 parts chloroform: 1 part isoamyl-alcohol was added to the mixture and the tube was centrifuged for 5 mins at 9.3 xg.

The supernatant was transferred into a fresh tube and 0.1 volumes of 7 M sodium acetate pH 5.2 and 2.5 volumes ice-cold 100% ethanol added onto the samples. The samples

were incubated at $-20\text{ }^{\circ}\text{C}$ for 30 mins and centrifuged for 10 mins at 9.3 xg. The supernatant was discarded and the pellet was washed with 70% ethanol. The sample was centrifuged for 10 mins at 9.3 xg and the supernatant discarded. The pellet was allowed to dry on a paper towel and re-suspended in 50 μl 1X TE. The DNA was stored at $4\text{ }^{\circ}\text{C}$ for future use.

2.2.8 Transformation of plasmid DNA into competent cells

Competent cells, which were prepared by Mr A. Faro, Department of Biotechnology, UWC, were thawed on ice for 5 mins. 10 μl ligation mixture or plasmid DNA was added to 50 μl of competent cells and the cells incubated on ice for 30 mins. The cells were heat-shocked at $42\text{ }^{\circ}\text{C}$ for 45 s and incubated on ice for a further 5 mins. 900 μl of prewarmed LB was added and the tubes were incubated at $37\text{ }^{\circ}\text{C}$ for 1 hour with shaking. 100 μl of the culture was plated on LB agar plates containing 100 $\mu\text{g}/\text{ml}$ ampicillin and incubated at $37\text{ }^{\circ}\text{C}$ overnight.

2.3 Expression and purification of the recombinant protein

2.3.1 Small-scale protein expression screen

Single colonies of *E.coli* BL21 cells transformed with expression vector were picked, inoculated in 6 ml LB containing 100 $\mu\text{g}/\text{ml}$ ampicillin and incubated at $37\text{ }^{\circ}\text{C}$ with shaking. After four hours two samples of 2 ml each were transferred into fresh tubes, and IPTG added to a final concentration of 0.1 mM (induced samples). Nothing was added to the remaining 2 ml sample (uninduced sample). Both the induced and the uninduced cultures were incubated at $37\text{ }^{\circ}\text{C}$ for a further 3 hours. The cells were harvested by

centrifugation at 15.7 xg for 10 mins. 40 µl of sample buffer was added to both the induced and the uninduced pellet and the protein was analysed on a 16% SDS PAGE gel (Section 2.5).

2.3.2 Large-scale expression of recombinant protein

Single colonies of *E.coli* BL21 cells transformed with expression plasmids were inoculated into 6 ml LB containing 100 µg/ml ampicillin and 34 µg/ml chloramphenicol and incubated at 37 °C with shaking. After 4 hours, 2 ml was used to inoculate 100 ml of either enriched media (LB) containing 100 µg/ml ampicillin and 34 µg/ml chloramphenicol. For ¹⁵N-labelling, proteins were expressed in minimal media in which NH₄Cl in M9 salts was substituted by ¹⁵NH₄Cl. The culture was incubated at 37 °C overnight with shaking. The following morning the overnight culture was scaled-up to 1000 ml by addition of 900 ml media containing the same concentration of antibiotics and incubated at 37 °C for six hours with shaking until the optical density at 550 nm reached between 0.4 and 0.6.

One hour prior to induction 100 µM ZnSO₄ was added for proper folding of the protein. Induction was carried out at 25 °C for 16 hours by addition of IPTG to a final concentration of 0.7 mM. Following induction the bacterial cells were recovered by centrifugation at 5000 g for 10 mins at 4 °C and the pellets stored at -20 °C until needed. After freezing the pellet was re-suspended in 20-25 ml lysis buffer. Lysis was carried out in three successive cycles of freezing at -70 °C for 5 mins, followed by thawing at 37 °C

for 5 mins. 0.02% of sodium azide was added to inhibit bacterial growth and the lysate was held at 4 °C until further purification.

2.3.3 Glutathione affinity purification of GST-fusion proteins

10 ml glutathione agarose beads were prepared by mixing 700 mg lyophilized beads with distilled water, and leaving it to swell overnight at 4 °C. After swelling the agarose beads were poured into a 20 ml disposable plastic column and washed thoroughly with equilibration buffer (PBS) to remove traces of lactose present in the lyophilized beads. For long-term storage the beads were stored at 4 °C in 1 M NaCl and 1 mM sodium azide. Prior to each purification, the column was washed with 3 column volumes (CV) of 2 M NaCl and equilibrated with 5 CV of 1 X PBS. 10 ml of the protein sample was added to the column and the flow through collected. The column was then washed with 5 CV of PBS containing 1% Triton X100 and the flow through collected. To elute retained fusion protein, 1 CV of elution buffer containing 10 mM glutathione in 50 mM Tris pH 9.5 was added to the column and the flow through collected in 10 ml fractions. Finally the column was washed with 5 CV of 2 M NaCl.

2.3.4 Cleavage of the GST-fusion proteins using 3C protease

3C protease from human rhinovirus (HRV 3C), recombinantly expressed as a GST-fusion protein, was a kind gift of James Ezenwa Onyemata in the Department of Biotechnology, UWC. 40 µl 3C protease, 0.001 M EDTA, 0.001 M DTT and 1% TRITON X100 were added to the recombinant protein which was transferred to dialysis tubing (MWCO 3500Da) and placed in 2000 ml cleavage buffer and incubated overnight at 4 °C with

stirring following cleavage, the target protein was separated from GST in a second round of glutathione affinity purification (see Section 2.3.3), with the target protein remaining in the flow through and GST and 3C protease being retained on the column.

2.3.5 Anion exchange chromatography

Anion ion exchange chromatography was carried out using a 1.6 ml column containing 20HQ POROS media (Amersham Bioscience) on a BioCad SprintTM perfusion chromatography system (Perspective Biosystems). The buffer used was 50 mM Tris-Cl, pH 7.0 flowing at a rate of 10 ml/min. The instrument was operated using a pre-programmed sequence comprising of a 10 column volumes (CV) equilibration step, followed by injection of the sample, followed by 10 CV wash step, followed by a 0-0.5 M NaCl gradient spanning 15 CV, followed by a final wash step consisting of 5 CV of 2 M NaCl. Eluted proteins were monitored using A₂₈₀ using an in-time UV detector and the NaCl concentration was monitored using an in-time conductivity meter. 1 ml fractions were collected using a GILSON® FC-203B automated fraction collector and the presence of eluted proteins was confirmed by analysing fractions on SDS-PAGE gel.

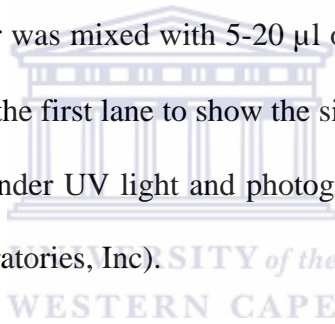
2.3.6 Size exclusion chromatography

Final purification (removal of residual GST) was performed using a 150 ml Sephacryl S100 column (Amersham Pharmacia Biotech) operated manually using a BioCad Sprint Perfusion chromatography system. The column was equilibrated with 1.5 CV of NMR buffer at a flow rate of 1.5 ml/min. Protein samples were concentrated to 1 ml using Viva Spin ultra-filtration devices (MWCO 3500 Da, Satorius Stedim Biotech S.A) and injected

into a 1 ml sample loop using a Hamilton 1 ml syringe. Fractions were collected using a GILSON® FC-203B automated fraction collector and the presence of eluted proteins was confirmed by analysing on SDS-PAGE gel.

2.4 Agarose gel electrophoresis of DNA

DNA was analysed by electrophoresis on 1% agarose gels. Gels were prepared by adding the required volume of 1 X TBE to the appropriate mass of electrophoresis grade agarose. The agarose was boiled and cooled to 55 °C followed by the addition of ethidium bromide to a final concentration of 0.5 µg/ml and poured onto a gel casting device. 0.5 µl of loading buffer was mixed with 5-20 µl of the DNA and loaded onto the gel. The marker was loaded in the first lane to show the sizes of the bands. The DNA was visualised by placing the gel under UV light and photographed using a ChemiDoc XRS Imager System (Bio-Rad Laboratories, Inc).



2.5 SDS-PAGE gel electrophoresis

Proteins were analysed by electrophoresis on 16% polyacrylamide gels using Laemmli's method (Laemmli, 1970). The separating gel was prepared from 8 ml 40% 37:5:1 polyacrylamide, 0.12 ml 10% APS, 0.21 ml 10% SDS, 5.25 ml separating buffer, 0.021 ml TEMED and the volume was made up to 20 ml using distilled water. The stacking gel was prepared from 1.5 ml 40% 37:5:1 polyacrylamide, 0.05 ml 10% APS, 0.1 ml 10% SDS, 2.5 ml stacking buffer, 0.02 ml TEMED and the volume was made up to 10 ml using distilled water.

Samples were mixed with equal volumes of 2X SDS sample buffer, incubated in a heat block at 100 °C for 10 mins and centrifuged for 10 mins at 9.3 xg. The samples were then electrophoresed at 10 V/cm using a Hoefer Mighty Small II gel electrophoresis system. Once the dye front had reached the end of the gel, the gel was removed from the caster and incubated in Coomassie staining solution for 30 mins. Thereafter it was transferred into Destaining solution until the background was clear.

2.6 Bradford Assay

Protein concentrations were determined using the Bradford Assay, using BSA (Bovine Serum Assay) as the standard. From a stock solution of 1 mg/ml BSA, a series of dilutions was made in the range 10 µg/ml to 50 µg/ml, using the same buffer as in the sample to be tested. The sample to be tested was diluted 1:1000 and 1:2000 dilutions, 200 µl of both dilutions of the sample and each dilution of the standard were added in duplicate to cuvettes. 200 µl of buffer was added in duplicate to serve as blank. The 5X Bradford Reagent was diluted in a 1:5 dilution in water and 1800 µl added to each cuvette. The samples were allowed to stand for 5 mins at room temperature. The absorbance was measured at 595 nm using the spectrophotometer. The average of each pair of duplicates were calculated and the standard curve plotted using Microsoft Excel. The absorbance at 280 nm (A_{280}) was measured using a NanoDrop ® ND 1000 spectrophotometer (Nano Drop technologies, Inc). A sample of 2 µl was used for each measurement. The spectrophotometer was calibrated using the same buffer as in the sample to be measured.

2.7 NMR analysis and characterisation of Zn²⁺ binding

2.7.1 Sample preparation

Samples were concentrated to 600 µl (2.805 mM) using Viva spin ultra-filtration devices (MWCO 3500 Da, Sartorius Stedim Biotech S.A) and 7% D₂O was used to act as a lock signal. Efficient suppression of the water resonance at 4.73 ppm was achieved using pre-saturation. NMR analysis was carried out in H₂O rather than D₂O because exchange of the labile amide protons would have resulted in suppression of their NMR resonances, which are required for ¹⁵N-HSQC experiments

2.7.2 NMR data collection and processing

All NMR spectra were recorded at 25 °C on the Varian Unity Inova 600 MHz spectroscopy in the Department of Chemistry at the University of Stellenbosch. Spectra were processed using NMRPipe (Delaglio *et al.*, 1995) and analysed using NMRView (Johnson, 2004).

2.7.3 Replacement of Zn²⁺ by ¹¹³Cd²⁺

50 µl of 50 mM ¹¹³Cd-EDTA was added to a 0.5 mM ¹⁵N-labelled protein sample, to a final concentration of 4 mM. The replacement of Zn²⁺ by Cd²⁺ was conducted by observing its effect on the ¹⁵N-HSQC spectrum of the protein.

2.7.4 pH sensitivity measurements

A series of NMR buffers was prepared with pH values 6.0, 5.8, 5.6, 5.4 and 5.2 respectively. A 600 µl NMR sample containing approximately 0.5 mM protein was dialysed against a 10-fold diluted NMR buffer and then 100 µl was added to 500 µl of

each buffer in the pH series, to produce five separate samples of 600 µl each. Each sample was transferred to a separate NMR buffer. 7% D₂O was added to serve as lock signal.

2.7.5 Prediction of protein parameters

Prediction of protein molecular weights, pI and nitrogen content were made using the online server Expasy Translate Tool (<http://au.expasy.org/cgi-bin/protparam>), see Appendix IV.



Chapter 3: Recombinant expression and purification of shortened RING finger domains

Previous analysis of a fragment of human RBBP6 containing the RING finger domain using NMR showed that the first 19 amino acids at the N-terminus were unfolded. Multiple resonances resulting from the structural heterogeneity of these residues led to obscuring of a number of structurally important resonances, hampering efforts to determine the structure of the domain. The aim of the work described in this chapter was to remove this unstructured region and produce two constructs shortened by 13 and 19 amino acid respectively. The constructs will be referred to as RING_sl (“RING_short-long”) and RING_ss (“RING_short-short”) respectively.

The two constructs were expressed as GST fusion proteins, using the pGEX-6P-2 vector system (Amersham Pharmacia Bioscience). The pGEX-6P-2 expression vector contains a *tac* promoter, which under IPTG induction drives the expression of recombinant proteins at high levels. The GST tag allows for affinity purification using a glutathione agarose column as well as improving the solubility of the target protein. The recognition site for 3C protease allows for separation of the target protein from GST. The expected amino acid sequences of the two shortened constructs following removal of GST is a domain shown in Appendix I.

3.1 Cloning of shortened RING constructs into the pGEX-6P-2 expression vector

3.1.1 PCR amplification of RING finger domains

Two new forward primers were synthesized to shorten the previous construct by 13 and 19 amino acids, respectively (see Fig 3.1). The reverse primer was the same as used

previously. Both forward primers incorporated *Bam* HI restriction sites and the reverse primer incorporated an *Xho* I restriction site. Both fragments were amplified by PCR using the original RING construct as a template, as described in Section 2.2.2. Fig 3.2 shows that both RING_sl and RING_ss fragments were successfully amplified.

3.1.2 Cloning of RING fragments into the pGEM-T Easy vector

The PCR products were cloned into the pGEM-T Easy TA cloning vector and transformed into competent *E.coli* MC1061 cells as described in Chapter 2. Five colonies were picked for each RING construct and a colony PCR using M13 primers was used to screen for recombinant colonies. The expected sizes of positive clones are 461 bp and 443 bp for RING_sl and RING_ss respectively, corresponding to the insert flanked by 100 bp on both ends. Positive clones for RING_sl can be seen in lanes 3,4 and 6 of Fig 3.3; a single positive clone for RING_ss appears in lane 8.

One colony from each of the positive clones was inoculated into enriched media for small scale DNA isolation as described in Section 2.3.7, and plasmid DNA was digested with *Bam* HI and *Xho* I to release the insert. The appearance of a fragment of the expected size (~261 bp) in lane 4 of Fig 3.4 shows that RING_sl was successfully cloned. The absence of similar fragments in lane 2 shows that cloning of the RING_ss was unsuccessful. The RING_sl restriction fragment was purified from the gel and cloned into the pGEX-6P-2 expression vector. Plasmid DNA was isolated as described in Section 2.3.7 and digested with *Bam* HI and *Xho* I to release the insert. Positive clones can be seen in lanes 2 to 4 and 6 of Fig 3.5.

Since cloning the RING_{ss} into pGEM-T Easy was unsuccessful, the PCR fragment was cloned directly into the pGEX-6P-2 expression vector. PCR amplified fragments were digested using *Bam* HI and *Xho* I restriction endonucleases, gel-purified using the GFX kit and cloned directly into pGEX-6P-2 expression vector. Isolation of plasmid DNA followed by digestion with *Bam* HI and *Xho* I restriction endonucleases revealed the presence of four positive clones (data not shown)

3.1.3 DNA sequencing

Four RING_{sl} and four RING_{ss} clones were sequenced. The sequences of both RING_{sl} and four RING_{ss} determined and analysed as described in Section 2.2.6. All RING_{sl} sequences were found to contain the same single mutation at position 219 of the query sequence. However, it is a silent mutation, since it replaces CAG with CAA, both of which code for glutamine (Q). The other mutation, which appears at position 235 of the 3' amplified sequence, was found to be a base-calling error on inspection of the sequencing trace (see Appendix II). All RING_{ss} sequences were 100% correct (see Appendix III).

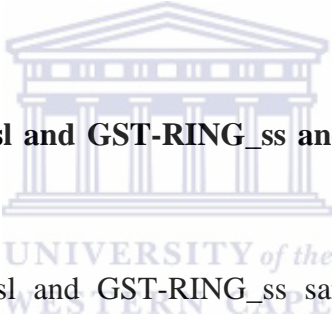
3.2 Expression and affinity purification of GST-RING_{sl} and GST-RING_{ss}

GST-RING_{sl} and GST-RING_{ss} plasmid constructs were transformed into *E.coli* BL21 competent cells and screened for expression using small-scale expression screen described in Section 2.3.1 Both GST-RING_{sl} (see Fig 3.6) and GST-RING_{ss} showed good expression relative to the uninduced samples. Large-scale expression and extraction

(Section 2.3.2) showed that both proteins were expressed at high levels in enriched media and were both found in the soluble fractions following extraction.

When expressed in minimal media, most of the protein was found in the insoluble fraction. However when the minimal media was supplemented with 100 μ M ZnSO₄, the protein was once again found at high levels in the soluble fractions. Fusion proteins were separated from cellular proteins using glutathione affinity chromatography as described in Section 2.3.3 Lanes 6 and 7 of Fig 3.7A provide an indication of the high levels of recovery of GST-RING_sl following affinity purification.

3.3 Cleavage of GST-RING_sl and GST-RING_ss and removal of GST by affinity chromatography

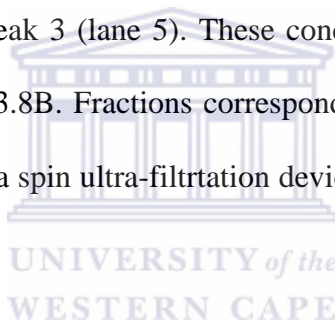


Affinity purified GST-RING_sl and GST-RING_ss samples were cleaved using 3C protease, and the GST was removed in a second round of glutathione agarose affinity purification. GST, GST-3C and uncleaved GST-RING were all retained by the column (free glutathione from the previous affinity step having been removed by dialysis prior to 3C cleavage), whereas RING_sl was collected in the flow through. As it can be seen from lanes 2-4 in Fig 3.7B RING_sl appears to be dimeric when visualised on SDS PAGE gel, something, which was also characteristic of the previous RING construct. RING_ss sometimes appears to be dimeric, sometimes monomeric (data not shown).

3.4 Final purification of RING_sl and RING_ss

3.4.1 Anion-exchange chromatography

Since the pI of GST and RING_sl are 5.0 and 4.7 respectively as determined by the ExPASy server (<http://www.expasy.org/tools/protparam.html>), it would be expected that both proteins would be strongly retained on an anion exchange column at pH 7.0, with RING_sl being slightly more strongly retained. A partially purified sample of RING_sl containing a small amount of GST was loaded onto the anion exchange column and eluted with a gradient of 0-0.5 M NaCl. The chromatogram in Fig 3.8A shows that both proteins were retained and that a clear separation was achieved between them with, surprisingly, RING_sl eluting near the beginning of the gradient (peak 2) and GST near the end (peak 3). From the apparent molecular weights it is clear that RING_sl elutes in Peak 2 (lane 2) and GST in Peak 3 (lane 5). These conclusions were confirmed by the SDS PAGE gel shown in Fig 3.8B. Fractions corresponding to peak 2 were pooled and concentrated to 1 ml using Viva spin ultra-filtration devices (MWCO 3500 Da, Sartorius Stedim Biotech S.A).



3.4.2 Size exclusion chromatography

Size exclusion chromatography using a 150 ml Sephacryl S100 column was used to remove residual GST and other contaminants, at the same time as exchanging the protein into NMR buffer. A clear separation between GST (Peak 1) and RING_sl (Peak 2) can be seen in Fig 3.8A, where the identities of the protein in each peak are confirmed by SDS PAGE gel analysis shown in Fig 3.9B. GST elutes earlier than RING_sl, as expected since it has a larger molecular weight than RING_sl (26.6 kD as opposed to 10.2296 kD). Similar results obtained for RING_ss are shown in Fig 3.10. Comparison of

Fig 3.9 and Fig 3.10 shows that RING_ss appears to be monomeric, whereas RING_sl appears to be dimeric, despite the fact that samples contained 1 mM DTT.

3.5 Determination of Protein concentration

After the final purification by size exclusion chromatography, fractions corresponding to RING_sl were pooled and concentrated down to a final volume of 600 μ l using Viva Spin Ultra filtration devices (MWCO 3500 Da, Sartorius Stedim Biotech S.A). The concentrated RING_sl sample is shown in Fig 3.11, where the extensive overloading shows that the protein is highly concentrated. 5 mM DTT was added to prevent the formation of inter-molecular disulphides bonds.

The final concentration of the RING_sl was determined using the Bradford Assay. Samples were prepared as described in Section 2.6 and absorbance readings at dilution factors of 1:1000 and 1:2000 were recorded at 595 nm. The absorbance readings (Table 3.1) for BSA were used to construct a standard curve (Fig 3.12) from which the concentration of RING_sl was determined. At 1:1000 dilution the absorbance of RING_sl was found to be 0.4685 (Table 3.1), which, using the standard curve, corresponds to ~28.6 μ g/ml, from which the original concentration was calculated to be:

$$\begin{aligned} C &= 28.6 \mu\text{g/ml} * 1000 \\ &= 28.6 \text{ mg/ml} \end{aligned}$$

At 1:2000 dilution the absorbance was found to be 0.237 (Table 3.1), which, using the standard curve corresponds to ~14.5 µg/ml, from which the original concentration was calculated to be:

$$\begin{aligned} C &= 14.5 \mu\text{g/ml} * 2000 \\ &= 28.9 \text{ mg/ml} \end{aligned}$$

Since the molecular weight of RING_sl is 10.2296 kD these correspond to molar concentrations of 2.79 mM and 2.82 mM respectively. We took the average of the two values, giving the concentration as 2.81 mM.

3.6 Calculation of the molar extinction coefficient

The absorbance at 280 nm (A_{280}) of the final NMR sample was determined using a NanoDrop® ND-1000 spectrophotometer (NanoDrop technologies Inc) and found to be 9.14 (see Fig 3.12). Note that the Nanodrop automatically adjust the optical path length so that the absorbance is within the linear range. However the output results is scaled so that it corresponds to as optical path length of 1cm. Using the Beer Lambert Law:

$$A_{280} = \epsilon Cl$$

And using the values $A_{280} = 9.14$, $C = 0.002805 \text{ M}$ and $L = 1 \text{ cm}$ (the optical path length), the molar extinction coefficient is calculated to be:

$$\epsilon = A_{280} / CL$$

$$\begin{aligned} &= 9.14 / (1 \text{ cm} * 0.002805 \text{ M}) \\ &= 3258 \text{ M}^{-1} \text{ cm}^{-1} \end{aligned}$$

This value can be compared to the extinction coefficient predicted by ExPASy server at <http://www.expasy.org/tools/protparam.html>, which is $2980 \text{ M}^{-1} \text{ cm}^{-1}$. The theoretical value was calculated by assuming that no cys residues appear as half cys, since 5 mM DTT was added to the final sample to reduce the disulphide bridges. Considering that RING_sl contains no Tryptophan residues which are the basis for the prediction, a 10% discrepancy between the observed and the predicted values of ϵ is probably within experimental errors.



Chapter 4: NMR analysis of Zn^{2+} coordination by the RBBP6 RING domain

4.1 Preliminary NMR analysis

Unlabelled and ^{15}N -labelled samples of RING_sl and RING_ss were produced as described in Chapter 3, and used to investigate the state of folding of both shortened domains using NMR. Chemical shifts of folded proteins are well dispersed relative to unfolded protein due to the presence of different chemical environments and shielding effects, particularly from the ring currents caused by aromatic side chains (Rehm *et al.*, 2002). The 1 dimensional (1D) spectrum of RING_sl shown in Fig 4.1A reveals that the protein is well folded, as indicated by the number of resonances that are shifted up-field into the region 8.5-10 ppm and down field into the region 0-1 ppm.

The 1D spectrum of the RING_ss shown in Fig 4.1B reveal that the protein is unfolded, as indicated by poorly dispersed amide backbone chemical shifts of the protons. The clustering of backbone H^{N} resonances around 8.3 ppm and poor dispersion of the resonances in the aliphatic region between 1.0 and -1.0 (Rehm *et al.*, 2002) also indicate that RING_ss is unfolded. To further confirm the folding and integrity of the two shortened RING constructs, ^{15}N -heteronuclear single quantum coherence spectra ^{15}N -HSQC were recorded. In a ^{15}N -HSQC spectrum each peak corresponds to the backbone NH group of a single amino acid, with the horizontal coordinate corresponding to the H^{N} chemical shift and the vertical coordinate corresponding to the chemical shift of the attached nitrogen. Exceptions are the pairs of peaks that correspond to side chain NH_2 groups of arginine and glutamine residues, which are found at the top right hand corner of the spectrum. Proline residues do not appear in the ^{15}N -HSQC spectrum, because they lack NH groups (Rehm *et al.*, 2002).

The ^{15}N -HSQC spectrum shown in Fig 4.2A confirms that RING_sl is folded as it is characterized by more peaks, which are well dispersed in both dimensions (Larsson *et al.*, 2003; Woestenenk *et al.*, 2003). In the ^1H dimension a number of resonances are shifted up field into the region to the left of 8.5 ppm. The resonances are very sharp, indicating that the protein tumbles rapidly in solution, which suggests that the protein adopts a globular shape. Unfolded proteins, on the other hand have broad lines as result of aggregation. The signals cluster around the ^1H frequency of 8.3 ppm with little dispersion to either sides. The ^{15}N -HSQC in Fig 4.2B confirms that RING_ss is unfolded (Larsson *et al.*, 2003).

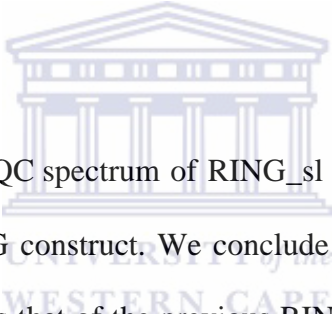
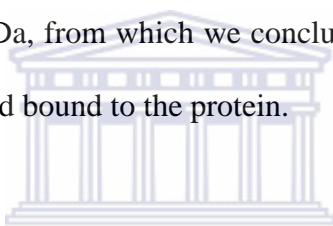


Fig 4.3 shows that the ^{15}N -HSQC spectrum of RING_sl (black) superimposes very well over that of the previous RING construct. We conclude from this that RING_sl adopts essentially the same structure as that of the previous RING construct, with the exception of the unstructured N-terminal amino acids. The RING_ss domain, on the other hand, is clearly unstructured and no further analysis of it was undertaken.

4.2 Investigation of Zn^{2+} binding using mass spectrometry

One of the primary aims of this work was to determine whether Zn^{2+} was required for the folding of the RBBP6 RING domain. The fact that protein expressed in the absence of Zn^{2+} (minimal media with no added Zn^{2+}) was predominantly insoluble whereas expression of protein in the presence of Zn^{2+} is soluble, suggested that Zn^{2+} was required.

In order to confirm this we first used mass spectrometry to investigate the mass of the protein. In the absence of Zn^{2+} ions RING_sl is expected to have a molecular weight of 10229.6 Da as determined by the on-line EXPASY server. However, since the sample was enriched with ^{15}N , and each molecule contained 122 nitrogen atoms, the size of the protein was expected to increase by 122 Da, giving an expected size of 10351.6 Da. Since the molecular weight of a single Zn^{2+} ion is 65.409 Da, with one Zn^{2+} bound the mass of the protein was expected to be 10417.009 Da, whereas with two ions bound it was expected to be 10482.418 Da. The mass found using Electro-spray mass spectrometry (see Fig 4.4) was 10349.0010 Da, from which we concluded that despite the use of mild conditions, no Zn^{2+} ion remained bound to the protein.



4.3 Investigation of Zn^{2+} binding using NMR

Cd^{2+} is known to replace Zn^{2+} in a number of proteins, with only minor effects on the structure of the protein (Hanzawa *et al.*, 2001; Houben *et al.*, 2005), However replacement leads to perturbation of the ^{15}N -HSQC spectrum of the proteins which therefore provides a convenient means of interpreting the exchange. Initially investigation of Zn^{2+} exchange by Cd^{2+} was unsuccessful, and no exchange was observed.

4.3.1 pH sensitivity measurements

Since the attempt to observe $\text{Cd}^{2+}/\text{Zn}^{2+}$ exchange was unsuccessful, it was decided to investigate the effect of pH on the stability of the Zn^{2+} -bound form of the protein. At high pH Zn^{2+} ions are tightly bound whereas below pH 5.5 Zn^{2+} coordination is expected to break down due to the sulphur atoms, which undergo oxidation due to DTT as a reducing agent (Davies *et al.*, 2005). 1D spectra of RING_sl were recorded in different pH buffers ranging from pH 6.0 to 5.2 as described in Section 2.7.4. As pH decreases steady loss of structure can be seen, in particular by a reduction in the size of amide resonance to the left of the 9 ppm and the methyl resonance at 0.1 ppm. At pH 5.2 the protein is almost completely unfolded. We concluded from our results that binding of Zn^{2+} was likely to be required for folding of the protein (see Fig 4.5).

4.3.2 Perturbation of ^{15}N -HSQC spectra

To confirm results obtained from pH investigation, that then folded protein bound Zn^{2+} ions, a second exchange experiment of Zn^{2+} by Cd^{2+} , was done again at pH 6.0. This time the results were conclusive. 25 μl of 50 mM ^{113}Cd -EDTA was added to a 2.805 mM ^{15}N -labelled RING_sl sample to a final concentration of 2 mM. Over a 2-week period a number of peaks disappeared and new peaks appeared. Fig 4.6 shows overlay spectra before (black) and after the exchange had taken place. Some peaks decayed/grew at a faster rate than others, suggesting that there are two binding sites with different affinities for Zn^{2+} and Cd^{2+} ions.

4.3.3 Refolding induced by Zn^{2+} and Cd^{2+}

After few weeks from the exchange experiment it was clear from the ^{15}N -HSQC spectra that both the Zn^{2+} and Cd^{2+} bound RING_sl samples stored at $4\text{ }^{\circ}\text{C}$ that they contained some unfolded protein. In an attempt to separate the unfolded protein from the folded protein, as well as to investigate whether the Cd^{2+} bound form would remain folded after the removal of excess ^{113}Cd -EDTA, both samples were subjected to size exclusion chromatography. NMR buffer was used without addition of either Zn^{2+} or Cd^{2+} . Fig 4.7 shows the appearance of a peak at the position expected for the bound protein (peak 2) and another broad peak (peak 1) suggesting that peak 1 and peak 2 correspond to the unfolded and folded protein respectively.

Fractions collected from both peaks were analysed by SDS PAGE gels, which confirmed that both peaks correspond to RING_sl protein. Fractions pooled from the narrow (peak 2) and the broad (peak 1) were analysed by NMR, the ^{15}N -HSQC spectrum shown in Fig 4.8 confirmed that they correspond to the folded and unfolded protein respectively. Similar results were obtained for Zn-bound form of RING_sl. After the addition of $\text{CdCl}_2/\text{ZnCl}_2$ to the unfolded protein (Fig 4.8B/E) the protein refolded (Fig 4.8C&F) as indicated by the appearance of more amide protons that are well dispersed on both dimensions. These investigations also reveal that RING_sl has strong affinity for $\text{Cd}^{2+}/\text{Zn}^{2+}$.

4.3.4 Direct detected ^{113}Cd NMR experiments

Since the coherence transfer between Cd^{2+} and RING_sl protons observed was not such as observed for CNOT4 and p44 (see Section 1.7), therefore Cd^{2+} -bound to the protein was observed using directly detected 1D ^{113}Cd spectrum. The 1D spectrum in Fig 4.9A contains three peaks: the peak at 556.6 ppm corresponds to the published chemical shift of ^{113}Cd -EDTA (Harris and Mann, 1978), where the spectrum is referenced to Di-methyl Cd^{2+} ($^{113}\text{CdMe}$) is at 0 ppm. When the spectrum is referenced to CdSO_4 is at 0 ppm, the two peaks on the left hand side of the spectrum correspond to chemical shifts in the vicinity of 720 ppm, which is consistent with the results obtained for CNOT4 and p44.

It was concluded that these two peaks correspond to the Cd^{2+} ions in the two sites of the protein. A series of 1D's recorded during the 2 week period of the exchange to occur (data not shown), showed build up of two peaks and decrease of ^{113}Cd -EDTA peak, confirming that the peaks correspond to Cd^{2+} ions bound to the protein. Two peaks correspond to Cd^{2+} exchanging into two sites in protein.

4.3.5 ^{113}Cd - ^1H coherence transfer experiments

The 1D directly detected spectrum shown in Fig 4.9A, indicated the frequency of the required carrier and the spectral width, to be able to locate the exchange on the ^{113}Cd - ^1H -HSQC spectrum. Using the new values, we were able to observe the coherence transfer from Cd^{2+} to protons in the protein.

The peaks at the top edge of the spectrum (Fig 4.9B) correspond to coherence transfer between $^{113}\text{Cd}^{2+}$ and the protons of EDTA. The same spectrum is shown in Fig 4.10,

which is the zoomed area of the two lines of peaks at around 720 ppm corresponding to coherence transfer between $^{113}\text{Cd}^{2+}$ and the H^β protons in the coordinating cysteine residues in RING_sl. As expected the proton chemical shifts are in the region 3 ppm, which is characteristic of cysteine H^β protons (http://www.bmrb.wisc.edu/ref_info/statel.html). Note that the projection of the $^{113}\text{Cd}^{2+}$ - ^1H -HSQC only the vertical axis gives the same spectrum as the 1D in (Fig 4.9A). Assignment of the side chains in the protein will allow us to determine which cysteine residues are bound to each Cd^{2+} .



Chapter 5: Discussion and conclusion

Sequence analysis of the RBBP6 RING finger domain indicated that the protein contains conserved cysteine residues, suggesting that like other RING finger domains it is possible that the RBBP6 RING finger might coordinate Zn^{2+} ions. It also pointed to the possibility that RBBP6 RING finger can also be classified as a member of the U box family, which do not require Zn^{2+} in order to fold, although they adopt the same structure as RING fingers. As shown the full RBBP6 RING finger construct domain contained an unstructured region at its N-terminus, and not suitable for further investigation of the domain using NMR. The aims for the study were therefore to truncate the N-terminal region and produce two constructs RING_sl and RING_ss, being shortened by 19 and 13 amino acid residues respectively, and to investigate the Zn^{2+} binding properties of the domain using NMR spectroscopy.

Both shortened constructs were successfully amplified, cloned and soluble protein expressed at high levels in rich media. However in minimal media soluble expression was only achieved following addition of $100\ \mu M$ $ZnSO_4$, which suggest that Zn^{2+} is required in order for the protein to fold. Purification was achieved by a combination of affinity, ion exchange and size exclusion chromatography. Protein samples suitable for NMR experiments were obtained at $0.5\ mM$ concentration.

Using both 1D proton and ^{15}N -HSQC spectra, RING_sl and RING_ss were found to be folded and unfolded respectively. We concluded from this that the boundary of the

domain falls between the two shortened constructs. The quality of the ^{15}N -HSQC spectrum of RING_sl was significantly better than the ^{15}N -HSQC spectrum of the previous construct, which will facilitate future structural work on the RBBP6 RING finger domain.

Using 1D proton spectra we showed that RING_sl unfolds rapidly as a function of pH as the pH drops below 6.0, which we interpreted as loosening of the coordination bonds. The addition of Cd^{2+} and Zn^{2+} to unfolded samples refolded the protein, confirming that Zn^{2+} is required for folding. Addition of ^{113}Cd -EDTA to the protein produced small chemical shift changes in the ^{15}N -HSQC spectrum, indicating that Cd^{2+} ions are able to replace Zn^{2+} ions without significantly changing the conformation of the protein. The changes took place over a time period of approximately 1 week for some residues, whereas other residues took almost 2 weeks to exchange fully, indicating that two different coordination sites may be involved. As observed the exchange was not the same for the two sites indicating the differences in affinity.

Using directly detected ^{113}Cd spectra we showed that Cd^{2+} binds to two different sites in the domain. This method, which has not been used previously to study metal binding in proteins, is easier and faster than recording ^{113}Cd indirectly detected experiments such as the ^{113}Cd - ^1H -HSQC. Using a ^{113}Cd - ^1H -HSQC experiment we were able to observe transfer of coherence between the Cd^{2+} and the $\text{H}\beta$ protons of the coordinating cysteines. The fact that the chemical shifts of the two Cd^{2+} ions are closer together than those observed for two other C4C4 RING fingers suggest that the chemical character of the two

coordination sites is even more similar than in those cases. Hence we conclude that the RBBP6 is more likely to be a C4C4 RING finger than a C3NC4 RING. However the question will remain unanswered until the structure of the domain has been determined at high resolution.

Assignments of the side chain chemical shifts of the RING finger is beyond the scope of this thesis, and so we were not able to determine the precise identities of the coordinating amino acid residues. However from the chemical shifts of the coordinating protons we can conclude that the majority of the coordinating residues are cysteines.



References

- Albert, T.K., Hanzawa, H., Legtenberg, Y.I., de Ruwe, M.J., van den Heuvel, F.A., Collart, M.A., Boelens, R., and Timmers, H.T. (2002). Identification of a ubiquitin-protein ligase subunit within the CCR4-NOT transcription repressor complex. *EMBO J* *21*, 355-364.
- Andersen, P., Kragelund, B.B., Olsen, A.N., Larsen, F.H., Chua, N.H., Poulsen, F.M., and Skriver, K. (2004). Structure and biochemical function of a prototypical Arabidopsis U-box domain. *J Biol Chem* *279*, 40053-40061.
- Aravind, L., and Koonin, E.V. (2000). The U box is a modified RING finger - a common domain in ubiquitination. *Curr Biol* *10*, R132-134.
- Birnboim, H.C., and Doly, J. (1979). A rapid alkaline extraction procedure for screening recombinant plasmid DNA. *Nucleic Acids Res* *7*, 1513-1523.
- Bottomley, M.J., Stier, G., Pennacchini, D., Legube, G., Simon, B., Akhtar, A., Sattler, M., and Musco, G. (2005). NMR structure of the first PHD finger of autoimmune regulator protein (AIRE1). Insights into autoimmune polyendocrinopathy-candidiasis-ectodermal dystrophy (APECED) disease. *J Biol Chem* *280*, 11505-11512.
- Capili, A.D., Edghill, E.L., Wu, K., and Borden, K.L. (2004). Structure of the C-terminal RING finger from a RING-IBR-RING/TRIAD motif reveals a novel Zn²⁺-binding domain distinct from a RING. *J Mol Biol* *340*, 1117-1129.
- Davies, A.M., Rasia, R.M., Vila, A.J., Sutton, B.J., and Fabiane, S.M. (2005). Effect of pH on the active site of an Arg121Cys mutant of the metallo-beta-lactamase from *Bacillus cereus*: implications for the enzyme mechanism. *Biochemistry* *44*, 4841-4849.
- Delaglio, F., Grzesiek, S., Vuister, G.W., Zhu, G., Pfeifer, J., and Bax, A. (1995). NMRPipe: a multidimensional spectral processing system based on UNIX pipes. *J Biomol NMR* *6*, 277-293.
- Dudev, T., and Lim, C. (2003). Principles governing Mg, Ca, and Zn binding and selectivity in proteins. *Chemical Reviews* *103*, 773-788.
- Dul, B.E., and Walworth, N.C. (2007). The plant homeodomain fingers of fission yeast Msc1 exhibit E3 ubiquitin ligase activity. *J Biol Chem* *282*, 18397-18406.
- Gao, S., and Scott, R.E. (2002). P2P-R protein overexpression restricts mitotic progression at prometaphase and promotes mitotic apoptosis. *J Cell Physiol* *193*, 199-207.

Gao, S., Witte, M.M., and Scott, R.E. (2002). P2P-R protein localizes to the nucleolus of interphase cells and the periphery of chromosomes in mitotic cells which show maximum P2P-R immunoreactivity. *J Cell Physiol* 191, 145-154.

Gourion-Arsiquaud, S., Chevance, S., Bouyer, P., Garnier, L., Montillet, J.L., Bondon, A., and Berthomieu, C. (2005). Identification of a Cd²⁺ - and Zn²⁺ -binding site in cytochrome c using FTIR coupled to an ATR microdialysis setup and NMR spectroscopy. *Biochemistry* 44, 8652-8663.

Hanzawa, H., de Ruwe, M.J., Albert, T.K., van Der Vliet, P.C., Timmers, H.T., and Boelens, R. (2001). The structure of the C4C4 ring finger of human NOT4 reveals features distinct from those of C3HC4 RING fingers. *J Biol Chem* 276, 10185-10190.

Harris, R.K., and Mann, B.E. (1978). *NMR and the Periodic Table*. Academic Press: London.

Houben, K., Wasielewski, E., Dominguez, C., Kellenberger, E., Atkinson, R.A., Timmers, H.T., Kieffer, B., and Boelens, R. (2005). Dynamics and metal exchange properties of C4C4 RING domains from CNOT4 and the p44 subunit of TFIIF. *J Mol Biol* 349, 621-637.

Huang, K., Johnson, K.D., Petcherski, A.G., Vandergon, T., Mosser, E.A., Copeland, N.G., Jenkins, N.A., Kimble, J., and Bresnick, E.H. (2000). A HECT domain ubiquitin ligase closely related to the mammalian protein WWP1 is essential for *Caenorhabditis elegans* embryogenesis. *Gene* 252, 137-145.

Huang, L., Kinnucan, E., Wang, G., Beaudenon, S., Howley, P.M., Huibregtse, J.M., and Pavletich, N.P. (1999). Structure of an E6AP-UbcH7 complex: insights into ubiquitination by the E2-E3 enzyme cascade. *Science* 286, 1321-1326.

Joazeiro, C.A., and Weissman, A.M. (2000). RING finger proteins: mediators of ubiquitin ligase activity. *Cell* 102, 549-552.

Johnson, B.A. (2004). Using NMRView to visualize and analyze the NMR spectra of macromolecules. *Methods Mol Biol* 278, 313-352.

Katoh, S., Hong, C., Tsunoda, Y., Murata, K., Takai, R., Minami, E., Yamazaki, T., and Katoh, E. (2003). High precision NMR structure and function of the RING-H2 finger domain of EL5, a rice protein whose expression is increased upon exposure to pathogen-derived oligosaccharides. *J Biol Chem* 278, 15341-15348.

Kellenberger, E., Dominguez, C., Fribourg, S., Wasielewski, E., Moras, D., Poterszman, A., Boelens, R., and Kieffer, B. (2005). Solution structure of the C-terminal domain of TFIIF P44 subunit reveals a novel type of C4C4 ring domain involved in protein-protein interactions. *J Biol Chem* 280, 20785-20792.

Kostic, M., Matt, T., Martinez-Yamout, M.A., Dyson, H.J., and Wright, P.E. (2006). Solution structure of the Hdm2 C2H2C4 RING, a domain critical for ubiquitination of p53. *J Mol Biol* 363, 433-450.

Krishna, S.S., Majumdar, I., and Grishin, N.V. (2003). Structural classification of Zn²⁺ fingers: survey and summary. *Nucleic Acids Res* 31, 532-550.

Kumar, S., Kao, W.H., and Howley, P.M. (1997). Physical interaction between specific E2 and Hect E3 enzymes determines functional cooperativity. *J Biol Chem* 272, 13548-13554.

Laemmli, U.K. (1970). Cleavage of structural proteins during the assembly of the head of bacteriophage T4. *Nature* 227, 680-685.

Larsson, G., Martinez, G., Schleucher, J., and Wijmenga, S.S. (2003). Detection of nanosecond internal motion and determination of overall tumbling times independent of the time scale of internal motion in proteins from NMR relaxation data. *J Biomol NMR* 27, 291-312.

Li, L., Deng, B., Xing, G., Teng, Y., Tian, C., Cheng, X., Yin, X., Yang, J., Gao, X., Zhu, Y., Sun, Q., Zhang, L., Yang, X., and He, F. (2007). PACT is a negative regulator of p53 and essential for cell growth and embryonic development. *Proc Natl Acad Sci U S A* 104, 7951-7956.

Pickart, C.M. (2001). Mechanisms underlying ubiquitination. *Annu Rev Biochem* 70, 503-533.

Pringa, E., Martinez-Noel, G., Muller, U., and Harbers, K. (2001). Interaction of the ring finger-related U-box motif of a nuclear dot protein with ubiquitin-conjugating enzymes. *J Biol Chem* 276, 19617-19623.

Pugh, D.J., Ab, E., Faro, A., Luty, P.T., Hoffmann, E., and Rees, D.J. (2006). DWNN, a novel ubiquitin-like domain, implicates RBBP6 in mRNA processing and ubiquitin-like pathways. *BMC Struct Biol* 6, 1.

Rehm, T., Huber, R., and Holak, T.A. (2002). Application of NMR in structural proteomics: screening for proteins amenable to structural analysis. *Structure* 10, 1613-1618.

Rodgers, K.K., Bu, Z., Fleming, K.G., Schatz, D.G., Engelman, D.M., and Coleman, J.E. (1996). A Zn²⁺-binding domain involved in the dimerization of RAG1. *J Mol Biol* 260, 70-84.

Sakai, Y., Saijo, M., Coelho, K., Kishino, T., Niikawa, N., and Taya, Y. (1995). cDNA sequence and chromosomal localization of a novel human protein, RBQ-1 (RBBP6), that binds to the retinoblastoma gene product. *Genomics* 30, 98-101.

Simons, A., Melamed-Bessudo, C., Wolkowicz, R., Sperling, J., Sperling, R., Eisenbach, L., and Rotter, V. (1997). PACT: cloning and characterization of a cellular p53 binding protein that interacts with Rb. *Oncogene 14*, 145-155.

Tatusova, T.A., and Madden, T.L. (1999). BLAST 2 Sequences, a new tool for comparing protein and nucleotide sequences. *FEMS Microbiol Lett 174*, 247-250.

Vo, L.T., Minet, M., Schmitter, J.M., Lacroute, F., and Wyers, F. (2001). Mpe1, a Zn²⁺ knuckle protein, is an essential component of yeast cleavage and polyadenylation factor required for the cleavage and polyadenylation of mRNA. *Mol Cell Biol 21*, 8346-8356.

Witte, M.M., and Scott, R.E. (1997). The proliferation potential protein-related (P2P-R) gene with domains encoding heterogeneous nuclear ribonucleoprotein association and Rb1 binding shows repressed expression during terminal differentiation. *Proc Natl Acad Sci U S A 94*, 1212-1217.

Woestenenk, E.A., Hammarstrom, M., Hard, T., and Berglund, H. (2003). Screening methods to determine biophysical properties of proteins in structural genomics. *Anal Biochem 318*, 71-79.

Yoshitake, Y., Nakatsura, T., Monji, M., Senju, S., Matsuyoshi, H., Tsukamoto, H., Hosaka, S., Komori, H., Fukuma, D., Ikuta, Y., Katagiri, T., Furukawa, Y., Ito, H., Shinohara, M., Nakamura, Y., and Nishimura, Y. (2004). Proliferation potential-related protein, an ideal esophageal cancer antigen for immunotherapy, identified using complementary DNA microarray analysis. *Clin Cancer Res 10*, 6437-6448.

Yurchenko, V., Xue, Z., and Sadofsky, M. (2003). The RAG1 N-terminal domain is an E3 ubiquitin ligase. *Genes Dev 17*, 581-585.

Zolk, O., Schenke, C., and Sarikas, A. (2006). The ubiquitin-proteasome system: focus on the heart. *Cardiovasc Res 70*, 410-421.

Appendix I: Amino acid sequence of the previous RBBP6 RING and shorted constructs.

Original RING construct

↓ ↓
GPLGSEEPSSSSEDDPIPDELLCLICKDIMTDAVVIPCCGNSYCDECIRTAL
LESDEHTCPTCHQNDVSPDALIANKFLRQAVNNFKNETGYTKRLRKQ

RING_sl

GPLGSEDDPIPDELLCLICKDIMTDAVVIPCCGNSYCDECIRTALLESEHTCPTCHQNDVSPDALIANKFLRQAVNNFKNETGYTKRLRKQ

RING_ss

GPLGSDELLCLICKDIMTDAVVIPCCGNSYCDECIRTALLESEHTCPTCHQNDVSPDALIANKFLRQAVNNFKNETGYTKRLRKQ

The original RING construct was shortened by 13 amino acid residue (red arrow), and by 19 amino acids (blue arrow) to produce RING_sl and RING_ss constructs respectively. The first 5 amino acids are artifacts produced by the pGEX-6P-2 expression system.

APPENDIX II: Sequence analysis of RING_sl cloned into pGEM-T Easy (sequenced by INQABA laboratory)

Forward RING_sl 1B T7

Alignment of RING finger short_long (Insilco) and sequenced RING finger short_long domain
 Query-Insilico sequence, and Sbjct-Sequenced sequence
 Score = 531 bits (276), Expect = 5e-148
 Identities = 278/279 (99%), Gaps = 0/279 (0%)
 Strand=Plus/Plus

```

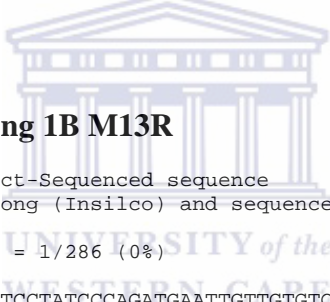
Query 7   SGATCCGAAGATGATCCTATCCAGATGAATTGTTGTGTCTCATCTGCAAGGATATTATG 66
          |||
Sbjct 57   SGATCCGAAGATGATCCTATCCAGATGAATTGTTGTGTCTCATCTGCAAGGATATTATG 116

Query 67   ACTGATGCTGTTGTGATTCCCTGCTGTGGAAACAGTTACTGTGATGAATGTATAAGAACA 126
          |||
Sbjct 117  ACTGATGCTGTTGTGATTCCCTGCTGTGGAAACAGTTACTGTGATGAATGTATAAGAACA 176

Query 127  GCACTCTGGAATCAGATGAGCACACATGTCCGACGTGTCATCAAAATGATGTTTCTCCT 186
          |||
Sbjct 177  GCACTCTGGAATCAGATGAGCACACATGTCCGACGTGTCATCAAAATGATGTTTCTCCT 236

Query 187  GATGCTTTAATTGCCAATAAATTTTACGACAGGCTGTAAATAACTTCAAAAATGAAACT 246
          |||
Sbjct 237  GATGCTTTAATTGCCAATAAATTTTACGACAGGCTGTAAATAACTTCAAAAATGAAACT 296

Query 247  GGCTATACAAAAGACTACGAAAACAGTGATAACTCGAG 285
          |||
Sbjct 297  GGCTATACAAAAGACTACGAAAACAGTGATAACTCGAG 335
  
```



Reverse RING finger short_long 1B M13R

Query-Insilico sequence, and Sbjct-Sequenced sequence
 Alignment of RING finger short_long (Insilco) and sequenced RING finger short_long,
 Score = 529 bits (275),
 Identities = 284/286 (99%), Gaps = 1/286 (0%)

```

Query 1   GAGGCCSGATCCGAAGATGATCCTATCCAGATGAATTGTTGTGTCTCATCTGCAAGGAT 60
          |||
Sbjct 415  GAGGCCSGATCCGAAGATGATCCTATCCAGATGAATTGTTGTGTCTCATCTGCAAGGAT 356

Query 61   ATTATGACTGATGCTGTTGTGATTCCCTGCTGTGGAAACAGTTACTGTGATGAATGTATA 120
          |||
Sbjct 355  ATTATGACTGATGCTGTTGTGATTCCCTGCTGTGGAAACAGTTACTGTGATGAATGTATA 296

Query 121  AGAACAGCACTCCTGGAATCAGATGAGCACACATGTCCGACGTGTCATCAAAATGATGTT 180
          |||
Sbjct 295  AGAACAGCACTCCTGGAATCAGATGAGCACACATGTCCGACGTGTCATCAAAATGATGTT 236

Query 181  TCTCCTGATGCTTTAATTGCCAATAAATTTTACGACAGGCTGTAAATAACTTCA-AAAA 239
          |||
Sbjct 235  TCTCCTGATGCTTTAATTGCCAATAAATTTTACGACAGGCTGTAAATAACTTCAAAAA 176

Query 240  TGAAACTGGCTATACAAAAGACTACGAAAACAGTGATAACTCGAG 285
          |||
Sbjct 175  TGAAACTGGCTATACAAAAGACTACGAAAACAGTGATAACTCGAG 130
  
```

Translation of experimental RING_sl sequence

ATA TGG CAG CTC GCA TGC TCC GGC GCC ATG CCG GCC GCC GGA ATT CGA TTG AGC GGA TCC
 I W Q L A C S G A M P A A G I R L S G S
 GAA GAT GAT CCT ATC CCA GAT GAA TTG TTG TGT CTC ATC TGC AAG GAT ATT ATG ACT GAT
 E D D P I P D E L L C L I C K D I M T D

GCT GTT GTG ATT CCC TGC TGT GGA AAC AGT TAC TGT GAT GAA TGT ATA AGA ACA GCA CTC
 A V V I P C C G N S Y C D E C I R T A L
 CTG GAA TCA GAT GAG CAC ACA TGT CCG ACG TGT CAT CAA AAT GAT GTT TCT CCT GAT GCT
 L E S D E H T C P T C H Q N D V S P D A
 TTA ATT GCC AAT AAA TTT TTA CGA CAA GCT GTA AAT AAC TTC AAA AAT GAA ACT GGC TAT
 L I A N K F L R Q A V N N F K N E T G Y
 ACA AAA AGA CTA CGA AAA CAG TGA TAA CTC GAG CGC CTC AAT CAC TAG TGA ATT CGC GGC
 T K R L R K Q * - L E R L N H * - I R G
 CGC CTG CAG GTC GAC CAT ATG GGA GAG CTC CCA ACG CGT TGG ATG CAT AGC TTG AGT ATT
 R L Q V D H M G E L P T R W M H S L S I

CAA- mutation CAG replaced by CAA, but still code for the same amino acid glutamine

Translation of expected RING_sl sequence

gag gcg gga tcc gaa gat gat cct atc cca gat gaa ttg ttg tgt ctc atc tgc aag gat
 E A G S E D D P I P D E L L C L I C K D
 att atg act gat gct gtt gtg att ccc tgc tgt gga aac agt tac tgt gat gaa tgt ata
 I M T D A V V I P C C G N S Y C D E C I
 aga aca gca ctc ctg gaa tca gat gag cac aca tgt ccg acg tgt cat caa aat gat gtt
 R T A L L E S D E H T C P T C H Q N D V
 tct cct gat gct tta att gcc aat aaa ttt tta cga cag gct gta aat aac ttc aaa aat
 S P D A L I A N K F L R Q A V N N F K N
 gaa act ggc tat aca aaa aga cta cga aaa cag tga taa ctc gag gcg gag
 E T G Y T K R L R K Q * * L E A E

Restriction sites are highlighted in red, CTCGAG- *Xho* I and GGATCC- *Bam* HI.

“Query” denotes the expected sequence, and “Sbjct” denotes the experimental sequence determined by sequencing sequence. A single silent mutation appears at position 219 of the Query sequence.

Appendix III: Sequence analysis of RING_ss cloned into pGEX-6P2 expression vector (sequenced by INQABA laboratory)

Forward RING_ss 1B M13R

Alignment of RING finger SS (Insilco) and sequenced RING finger SS,
 Query-Insilico sequence, sbjct: sequenced sequence.
 Score = 498 bits (259), Identities = 259/259 (100%), Gaps = 0/259 (0%)

```

Query 9   ATCCGATGAATTGTTGTGTCTCATCTGCAAGGATATTATGACTGATGCTGTTGTGATTCC 68
Sbjct 49   ATCCGATGAATTGTTGTGTCTCATCTGCAAGGATATTATGACTGATGCTGTTGTGATTCC 108

Query 69   CTGCTGTGGAAACAGTTACTGTGATGAATGTATAAGAACAGCACTCCTGGAATCAGATGA 128
Sbjct 109   CTGCTGTGGAAACAGTTACTGTGATGAATGTATAAGAACAGCACTCCTGGAATCAGATGA 168

Query 129   GCACACATGTCCGACGTGTCTCATCAAATGATGTTTCTCCTGATGCTTTAATTGCCAATAA 188
Sbjct 169   GCACACATGTCCGACGTGTCTCATCAAATGATGTTTCTCCTGATGCTTTAATTGCCAATAA 228

Query 189   ATTTTACGACAGGCTGTAAATAACTTCAAAAATGAACTGGCTATACAAAAGACTACG 248
Sbjct 229   ATTTTACGACAGGCTGTAAATAACTTCAAAAATGAACTGGCTATACAAAAGACTACG 288

Query 249   AAAACAGTGATAACTCGAG 267
Sbjct 289   AAAACAGTGATAACTCGAG 307

```

Reverse RING_ss 1B M13R

Alignment of RING finger SS (Insilco) and sequenced RING finger SS,
 Query-Insilco sequence, sbjct: sequenced sequence.
 Score = 504 bits (262), Identities = 262/262 (100%), Gaps = 0/262 (0%)

```

Query 6   SGGATCCGATGAATTGTTGTGTCTCATCTGCAAGGATATTATGACTGATGCTGTTGTGAT 65
Sbjct 311  SGGATCCGATGAATTGTTGTGTCTCATCTGCAAGGATATTATGACTGATGCTGTTGTGAT 252

Query 66   TCCCTGCTGTGGAAACAGTTACTGTGATGAATGTATAAGAACAGCACTCCTGGAATCAGA 125
Sbjct 251   TCCCTGCTGTGGAAACAGTTACTGTGATGAATGTATAAGAACAGCACTCCTGGAATCAGA 192

Query 126   TGAGCACACATGTCCGACGTGTCTCATCAAATGATGTTTCTCCTGATGCTTTAATTGCCAA 185
Sbjct 191   TGAGCACACATGTCCGACGTGTCTCATCAAATGATGTTTCTCCTGATGCTTTAATTGCCAA 132

Query 186   TAAATTTTACGACAGGCTGTAAATAACTTCAAAAATGAACTGGCTATACAAAAGACT 245
Sbjct 131   TAAATTTTACGACAGGCTGTAAATAACTTCAAAAATGAACTGGCTATACAAAAGACT 72

Query 246   ACGAAAAACAGTGATAACTCGAG 267
Sbjct 71   ACGAAAAACAGTGATAACTCGAG 50

```

Translation of experimental RING_ss sequence

```

gga gcg agg aca aca caa cac att gca tcg atg ccc cgc ctc tcg ttt caa acg tcg ccg gtg ggc
G A R T T Q H I A S M P R L S F Q T S P V G
ttt gag ggg ggt ggc ggg ggg cgc gtg ggc tgg caa gcc acg ttt ggt ggt ggc Gac cat cct cca
F E G G G G R V G W Q A T F G G G D H P P
aaa tcg gat ctg gaa gtt ctg ttc cag ggg ccc ctg gga tcc gat gaa ttg ttg tgt ctc atc tgc

```

```

K S D L E V L F Q G P L G S D E L L C L I C
aag gat att atg act gat gct gtt gtg att ccc tgc tgt gga aac agt tac tgt gat gaa tgt ata
K D I M T D A V V I P C C G N S Y C D E C I
aga aca gca ctc ctg gaa tca gat gag cac aca tgt ccg acg tgt cat caa aat gat gtt tct cct
R T A L L E S D E H T C P T C H Q N D V S P
gat gct tta att gcc aat aaa ttt tta cga cag gct gta aat aac ttc aaa aat gaa act ggc tat
D A L I A N K F L R Q A V N N F K N E T G Y
aca aaa aga cta cga aaa cag tga taa ctc gag cgg ccg cat cgt gac tga ctg acg atc tgc ttc
T K R L R K Q - - L E R P H R D - L T I C F
gcg cgt ttc ggt gatg
A R F G D

```

Translation of expected RING_ss sequence

```

gag gcg gga tcc gat gaa ttg ttg tgt ctc atc tgc aag gat att atg act gat gct gtt gtg att
E A G S D E L L C L I C K D I M T D A V V I
ccc tgc tgt gga aac agt tac tgt gat gaa tgt ata aga aca gca ctc ctg gaa tca gat gag cac
P C C G N S Y C D E C I R T A L L E S D E H
aca tgt ccg acg tgt cat caa aat gat gtt tct cct gat gct tta att gcc aat aaa ttt tta cga
T C P T C H Q N D V S P D A L I A N K F L R
cag gct gta aat aac ttc aaa aat gaa act ggc tat aca aaa aga cta cga aaa cag tga taa ctc
Q A V N N F K N E T G Y T K R L R K Q * * L
gag gcg gag
E A E

```

“Query” denotes the expected sequence, and “Sbjct” denotes the experimental sequence determined by sequencing sequence. The experimental and expected sequences are in 100% agreement.

Appendix IV: Prediction of protein parameters

A.Parameters for RING_sl

ProtParam
User-provided sequence:

10 20 30 40
 50 60
 GPLGSEDDPI PDELLCLICK DIMTDAVVIP CCGNSYCDEC IRTALLESDE HTCPTCHQND
 70 80 90
 VSPDALIANK FLRQAVNNFK NETGYTKRLR KQ

Please note the modified algorithm for extinction coefficient.

Number of amino acids: 92

Molecular weight: 10229.6

Theoretical pI: 4.67

Amino acid composition:

Ala (A) 5 5.4% Arg (R) 4 4.3% Asn (N) 6 6.5% Asp (D) 9 9.8% Cys (C) 8
 8.7% Gln (Q) 3 3.3% Glu (E) 6 6.5% Gly (G) 4 4.3% His (H) 2 2.2% Ile (I)
 6 6.5% Leu (L) 9 9.8% Lys (K) 5 5.4% Met (M) 1 1.1% Phe (F) 2 2.2% Pro
 (P) 6 6.5% Ser (S) 4 4.3% Thr (T) 6 6.5% Trp (W) 0 0.0% Tyr (Y) 2 2.2%
 Val (V) 4 4.3% Asx (B) 0 0.0% Glx (Z) 0 0.0% Xaa (X) 0 0.0%

Total number of negatively charged residues (Asp + Glu): 15

Total number of positively charged residues (Arg + Lys): 9

Atomic composition:

Carbon	C		435
Hydrogen	H	698	
Nitrogen	N		122
Oxygen	O		144
Sulfur	S		9



Formula: C435H698N122O144S9

Total number of atoms: 1408

Extinction coefficients:

This protein does not contain any Trp residues. Experience shows that this could result in more than 10% error in the computed extinction coefficient.

Extinction coefficients are in units of M⁻¹ cm⁻¹, at 280 nm measured in water.

Ext. coefficient 3480

Abs 0.1% (=1 g/l) 0.340, assuming ALL Cys residues appear as half cystines

Ext. coefficient 2980

Abs 0.1% (=1 g/l) 0.291, assuming NO Cys residues appear as half cystines

Estimated half-life:

The N-terminal of the sequence considered is G (Gly).

The estimated half-life is: 30 hours (mammalian reticulocytes, in vitro).

>20 hours (yeast, in vivo).

>10 hours (Escherichia coli, in vivo).

Instability index:

The instability index (II) is computed to be 38.52
This classifies the protein as stable.

Aliphatic index: 81.63

Grand average of hydropathicity (GRAVY): -0.376

B.Parameters for RING_ss

ProtParam

User-provided sequence:

```
          10          20          30          40
50
GPLGSDELLC LICKDIMTDA VVIPCCGNSY CDECIRTALL ESDEHTCPTC HQNDVSPDAL
          70          80
IANKFLRQAV NNFKNETGYT KRLRKQ
```

Please note the modified algorithm for extinction coefficient.

Number of amino acids: 86

Molecular weight: 9562.9

Theoretical pI: 5.18

Amino acid composition:

Ala (A) 5 5.8% Arg (R) 4 4.7% Asn (N) 6 7.0% Asp (D) 7 8.1% Cys (C) 8
9.3% Gln (Q) 3 3.5% Glu (E) 5 5.8% Gly (G) 4 4.7% His (H) 2 2.3% Ile (I)
5 5.8% Leu (L) 9 10.5% Lys (K) 5 5.8% Met (M) 1 1.2% Phe (F) 2 2.3% Pro
(P) 4 4.7% Ser (S) 4 4.7% Thr (T) 6 7.0% Trp (W) 0 0.0% Tyr (Y) 2 2.3%
Val (V) 4 4.7% Asx (B) 0 0.0% Glx (Z) 0 0.0% Xaa (X) 0 0.0%

Total number of negatively charged residues (Asp + Glu): 12

Total number of positively charged residues (Arg + Lys): 9

Atomic composition:

Carbon	C	406
Hydrogen	H	656
Nitrogen	N	116
Oxygen	O	132
Sulfur	S	9

Formula: C406H656N116O132S9

Total number of atoms: 1319

Extinction coefficients:

This protein does not contain any Trp residues. Experience shows that this could result in more than 10% error in the computed extinction coefficient.

Extinction coefficients are in units of M⁻¹ cm⁻¹, at 280 nm measured in water.

Ext. coefficient 3480

Abs 0.1% (=1 g/l) 0.364, assuming ALL Cys residues appear as half cystines

Ext. coefficient 2980

Abs 0.1% (=1 g/l) 0.312, assuming NO Cys residues appear as half cystines

Estimated half-life:

The N-terminal of the sequence considered is G (Gly).

The estimated half-life is: 30 hours (mammalian reticulocytes, in vitro).

>20 hours (yeast, in vivo).

>10 hours (Escherichia coli, in vivo).

Instability index:

The instability index (II) is computed to be 37.25

This classifies the protein as stable.

Aliphatic index: 82.79

Grand average of hydropathicity (GRAVY): -0.295





UNIVERSITY *of the*
WESTERN CAPE

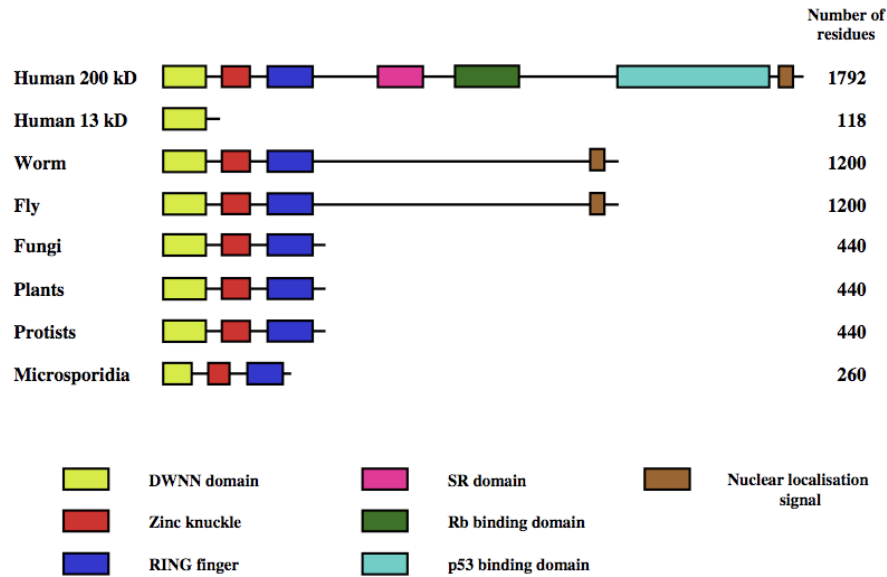


Figure 1.1 Schematic representations of the domain structure of RBBP6 homologues from different species. The RBBP6 protein consists of an N-terminal domain (DWNN), a zinc finger, and a RING finger domain, which are present as a single copy transcript in all complete eukaryotic genomes analysed to date including the parasite single celled *Encephalitozoon cuniculi*. In vertebrates and insects, the RBBP6 includes a long C-terminal extension, which includes an Rb-binding domain, a p53-binding domain, an SR domain and a nuclear localisation domain. Vertebrates also contain a short form, which consists of the N-terminal (DWNN) domain (figure adapted from Pugh *et al.*, 2006).

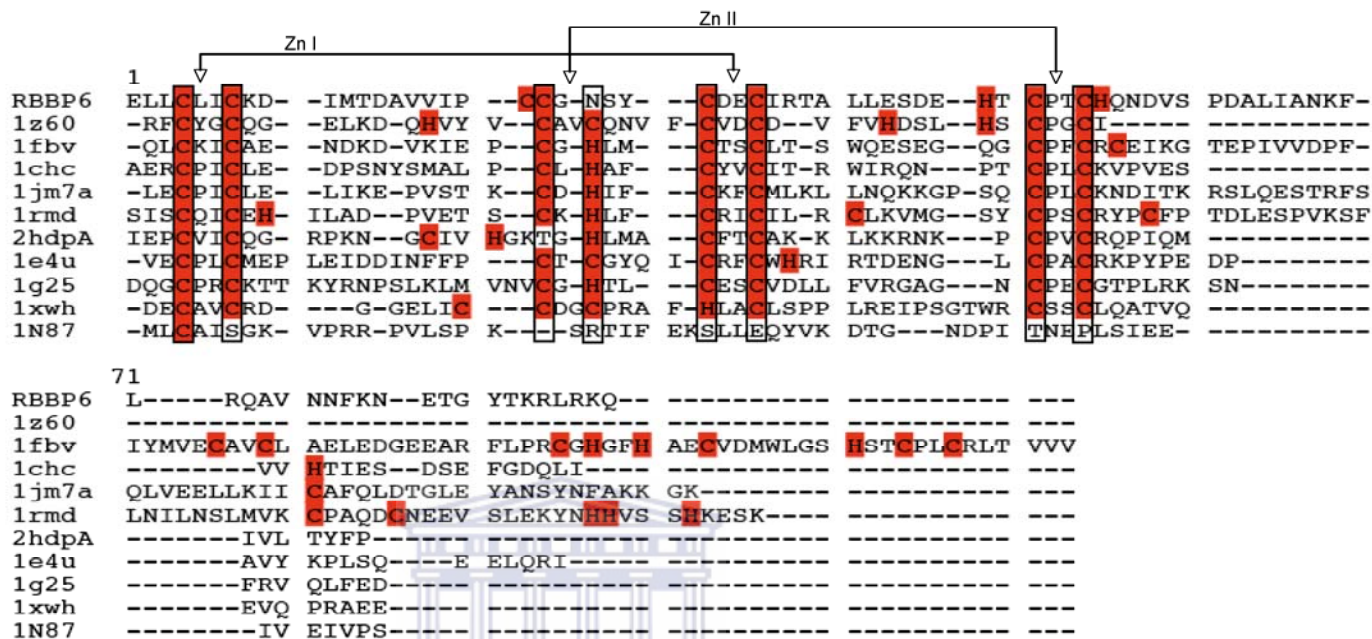


Figure 1.2 Alignment of RBBP6 RING finger against a number of RING finger and RING finger-like proteins. Cysteine and histidine residues coordinating Zn^{2+} are indicated in rectangles. The two sites coordinating Zn^{2+} are indicated by arrows. Included are: C3HC4 RING fingers MAT1 (1g25, res 1-65), RAG1 (1rmd, res 1-61), c-Cbl (1fbv, res 1-154), IEEHV (1chc, 1-68), and BRCA1 (1jm7a, 1-112); C4C4 RING fingers CNOT4 (1e4u, res 1-78) and p44 (1z60, res 1-59); C3HHC3 (RING-H2) EL5 (1iym, res 1-55); C4HC3 PHD finger (1xwh, res 1-66), C2H2C4 Hdm2 (2hdpA, res 1-63); U box (1n87, RES 1-56). In the U box domain, cysteine or histidine zinc binding residues are replaced by other residues. As can be seen from the alignment, RBBP6 RING is either a C4C4 RING finger or a novel C3NC4 RING finger. (Alignment created using Clustal X and edited using Seaview, sequences are referenced by their PDB accession numbers).

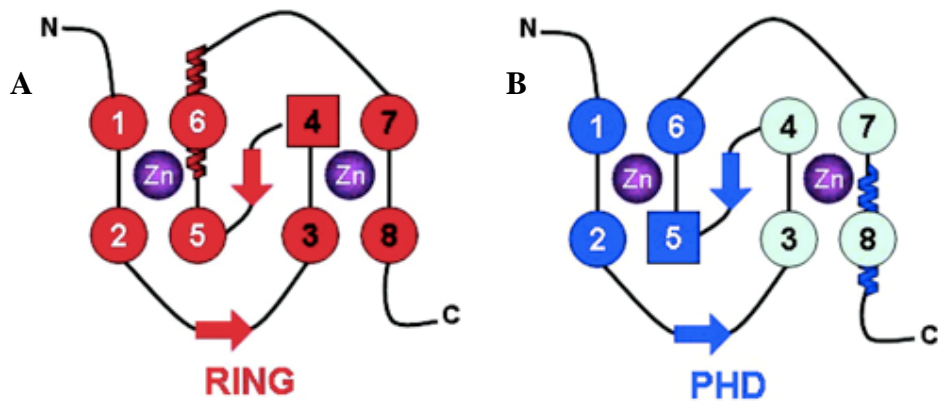


Figure 1.3 Schematic representation of the zinc coordination in RING finger and PHD domains. Zn I is coordinated by cysteine or histidine residues 1, 2, 5 and 6, and Zn II by residues 4, 3, 7 and 8, forming a cross-braced pattern. Cysteine residues are shown in circles and the histidine residues are shown in squares. The PHD and RING fingers have identical topology but differ in the arrangement of the secondary structure, with the α -helix forming part of the first zinc coordination site in the RING and the second coordination site in the PHD (figure adapted from Bottomley *et al.*, 2005).

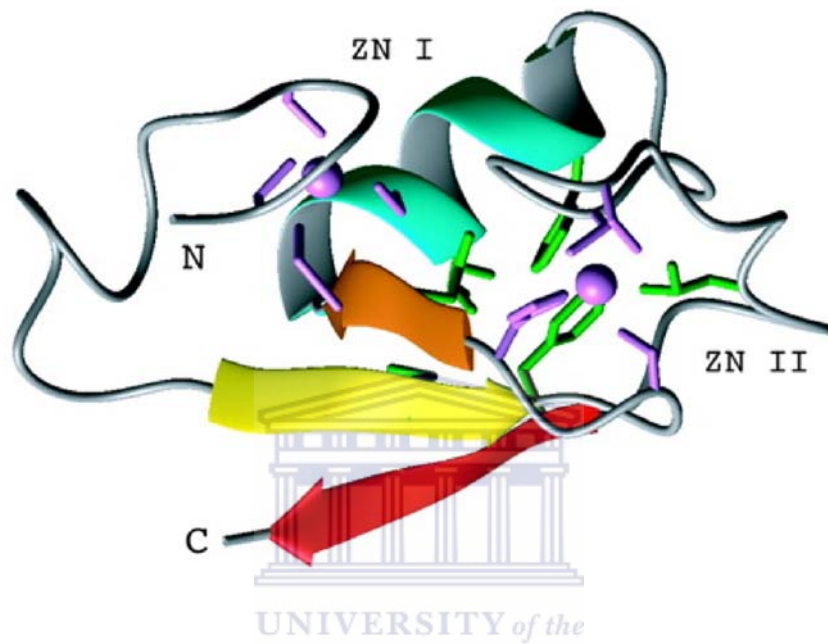


Figure 1.4 3D Structure of the MAT1 C3HC4 RING finger. The structure is stabilised by two zinc ions (indicated by magenta spheres). The secondary structure consists of a three-stranded anti-parallel β -sheet (shown in red, yellow and orange) and a single α -helix (blue), linked by loops (grey) (figure adapted from Kellenberger *et al.*, 2005)

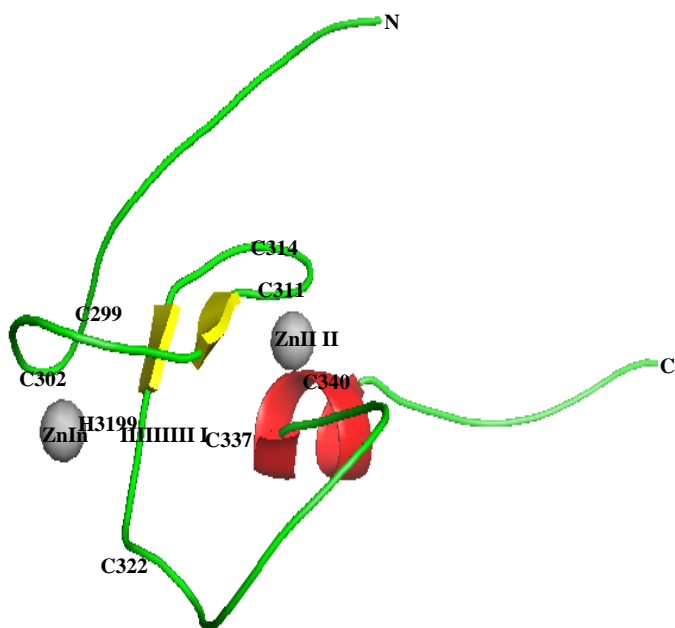


Figure 1.5 Cartoon representation of a 3D structure of the PHD from the AIRE1 (PDB: 1XWH). Zn I is coordinated by Cys299, Cys302, His319 and Cys322 and Zn II by Cys311, Cys314, Cys337 and Cys340, in a cross-braced manner. Zn is shown in grey spheres, β strands are shown in yellow, the α helix is shown in red (figure created using Pymol).

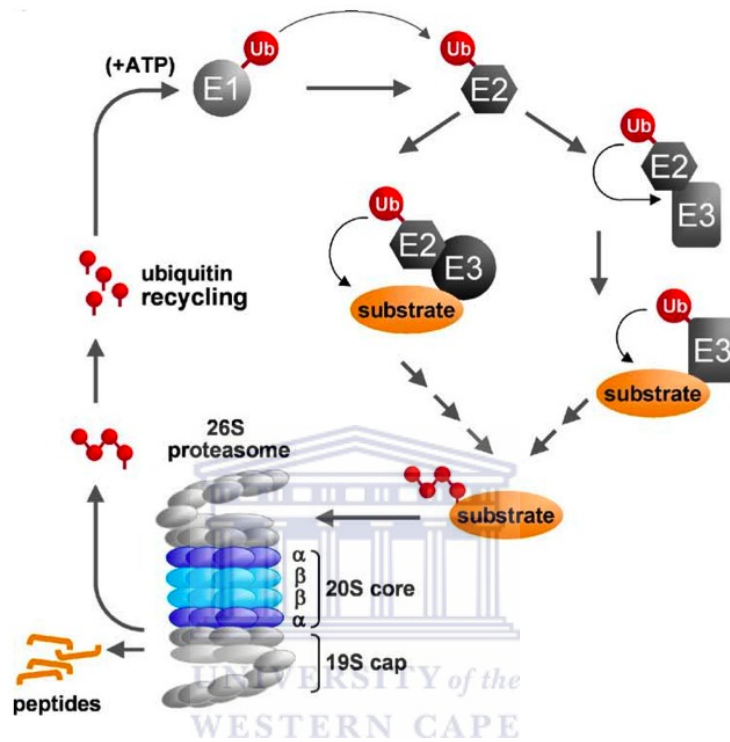


Figure 1.6 The ubiquitin-proteasome pathway. Ubiquitination proceeds in three steps: E1 first activates ubiquitin and then transfer it to E2. In the final step ubiquitin is either conjugated directly to the substrate from E2 (indicated with a circle) or a thiol ester bond is formed between the E2 and E3 enzymes before ubiquitin can be conjugated to the substrate (indicated with a square) depending on the class of E3 ubiquitin ligase catalysing the reaction. After formation of the polyubiquitin chain the target protein is degraded in the 26S proteasome and ubiquitin is recycled (figure adapted from Zolk *et al.*, 2006).

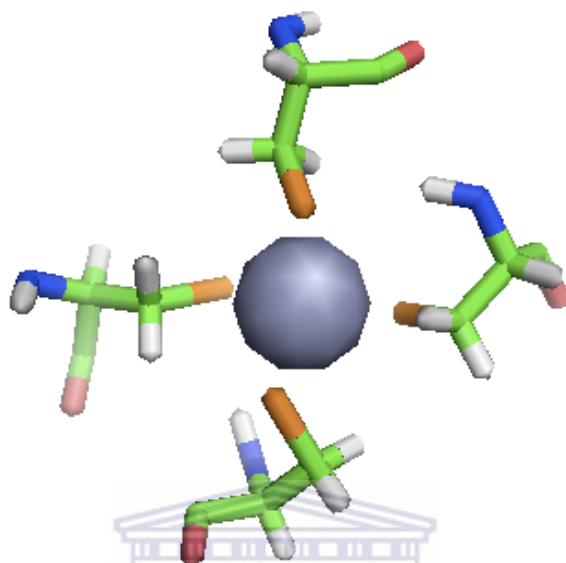


Figure 1.7 Tetrahedral coordination found in RING finger proteins. Section taken from site 2 of C4C4 CNOT4 RING finger (PDB:1e4u). Zn II is coordinated by four cysteine residues through the sulphur atoms. The atoms are coloured as follows, carbons (green), oxygen (red), hydrogen (grey), nitrogen (blue) and sulphur (orange). (figure created using Pymol).

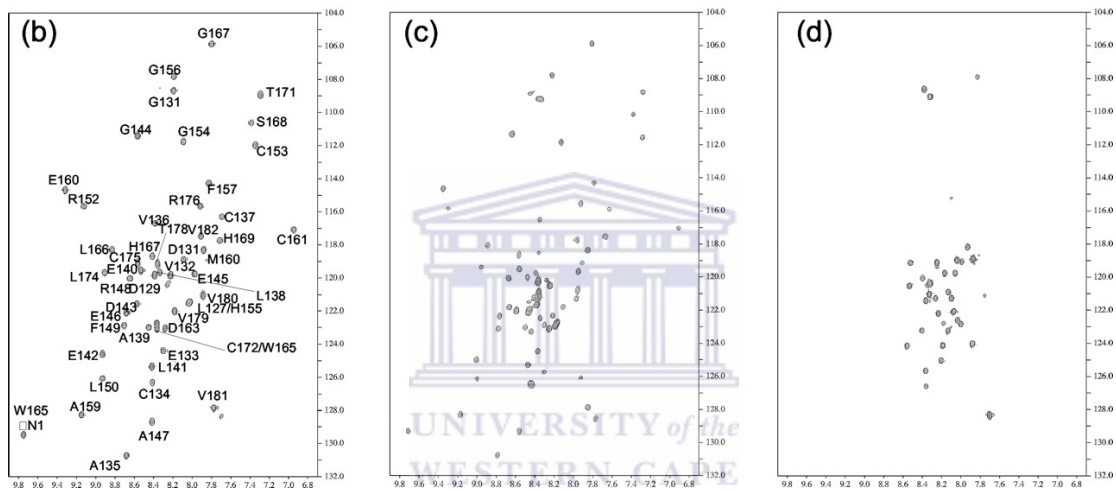
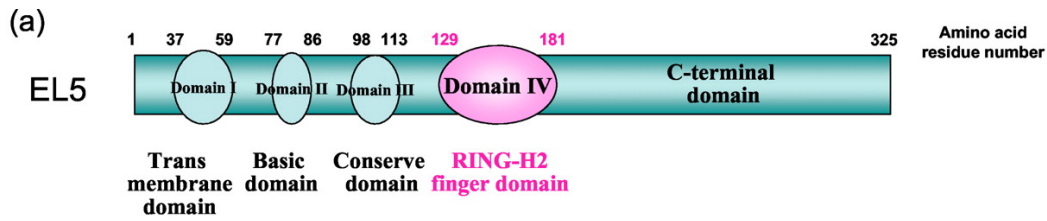


Figure 1.8 RING-H2 domain from EL5 requires Zn^{2+} in order to fold. The domain structure of EL5 (a), including the RING-H2 domain (residues 129-181). The domain is folded in the presence of zinc (b), but the addition of EDTA to chelate Zn^{2+} unfolds the protein (d). The addition of excess Zn^{2+} refolds the protein (c), indicating that the protein requires Zn^{2+} in order to fold (figure adapted from Katoh *et al.*, 2003).

(a)

QuickTime™ and a
TIFF (LZW) decompressor
are needed to see this picture.

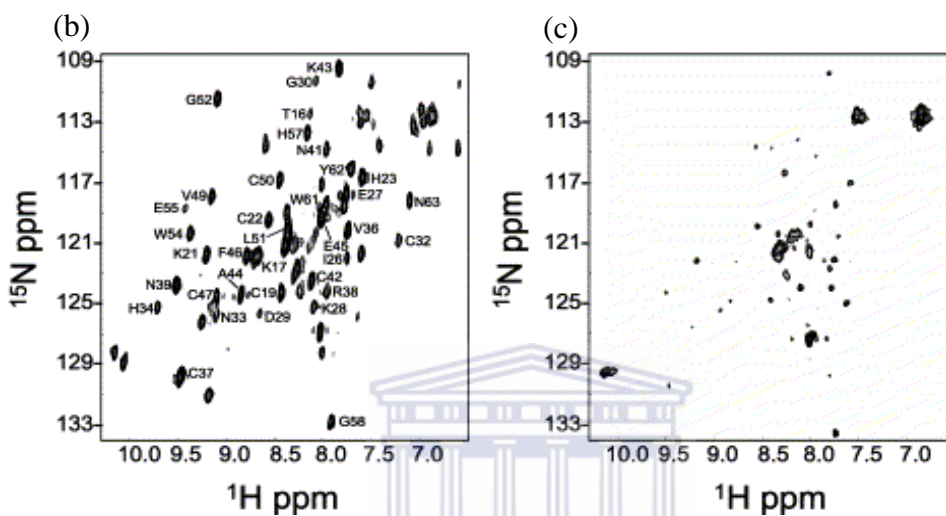


Figure 1.9 RING2 from HHARI requires Zn^{2+} in order to fold. (a) HHARI contains two RING finger domains (RING1 and RING 2) separated by an “In Between RING” domain (IBR). When expressed in the presence of zinc RING2 is folded (b), whereas when expressed in the absence of zinc it is unfolded (c) (^{15}N -HSQC spectra adapted from Capili *et al.*, 2004).

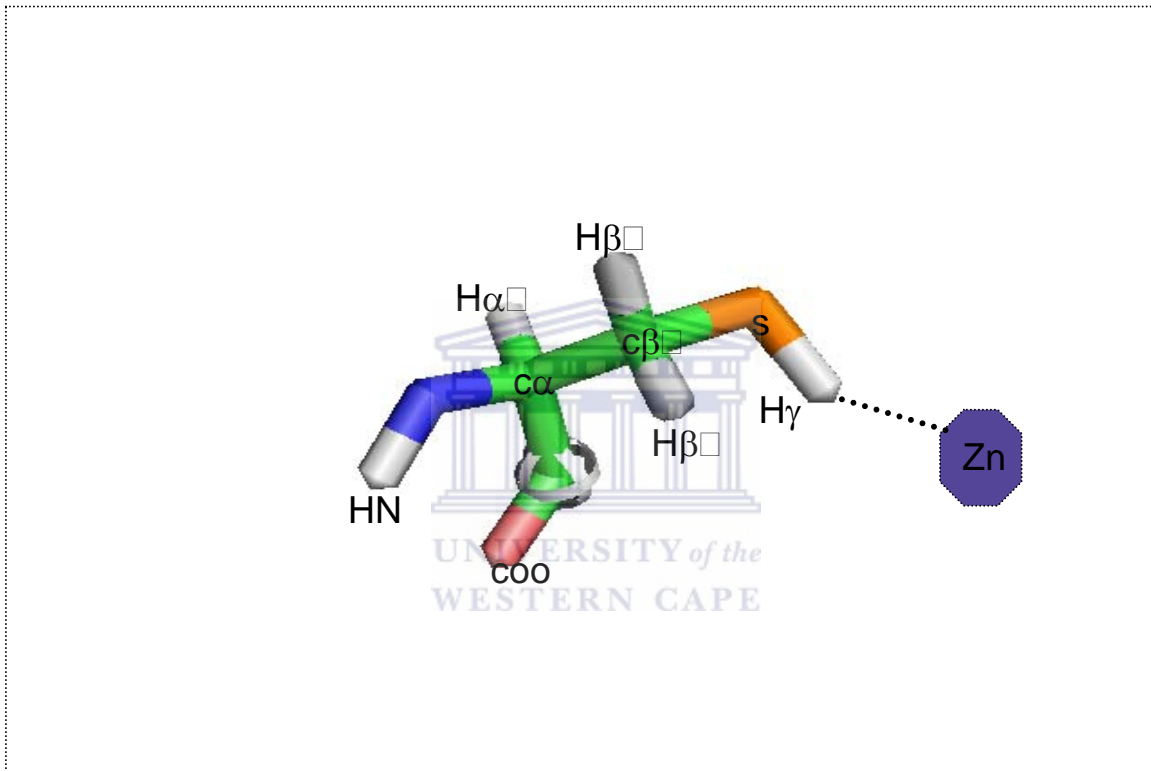


Figure 1.10 Coordination of Zn^{2+} by cysteine residues. The H^β protons are separated from the metal ion by three covalent bonds and the coordination bond. (Picture created using Pymol)

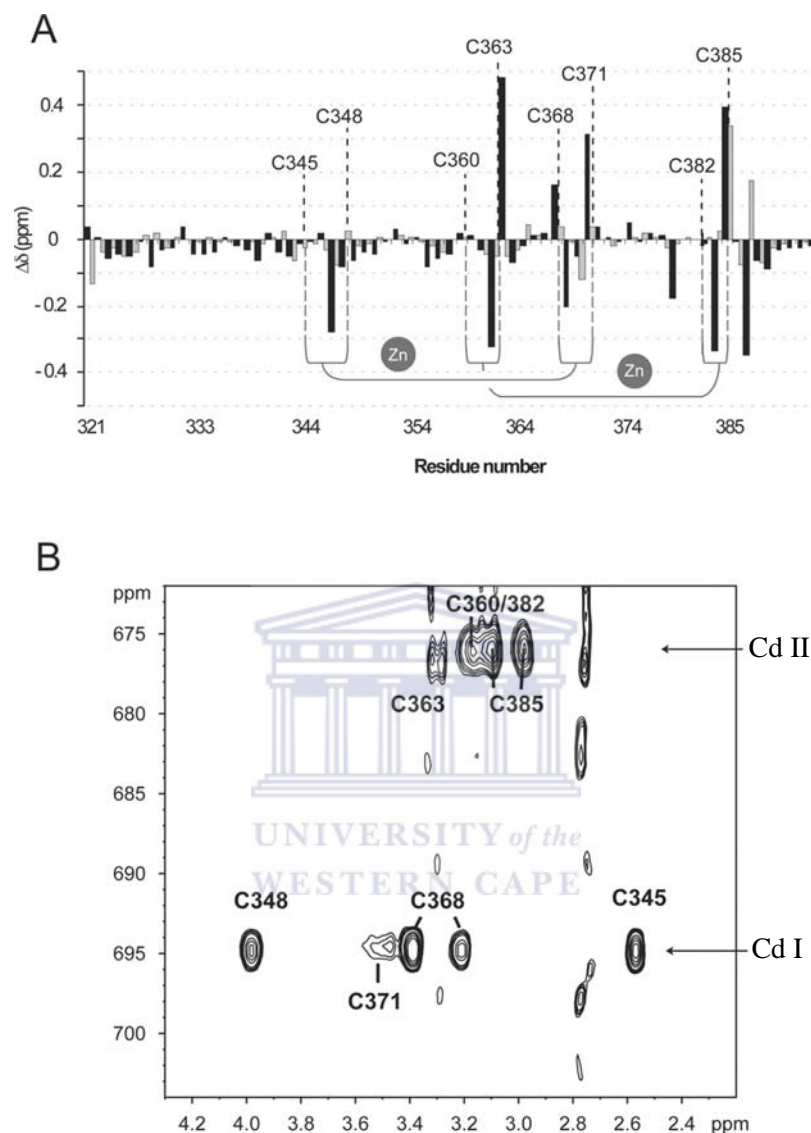


Figure 1.11 Determination of zinc coordinating residues by replacement of zinc with ^{113}Cd in the p44 RING domain. (A) Chemical shifts differences of the amide protons and nitrogen's of the p44 C4C4 RING domain following exchange of Zn^{2+} by Cd^{2+} showing (B), ^{113}Cd -HSQC spectrum, showing that Zn I and Zn II are coordinated in a cross-brace manner by Cys (348, 368, 371 and 345) and Cys (363, 360, 382, and 385) respectively (figure adapted from Kellenberger *et al.*, 2005).

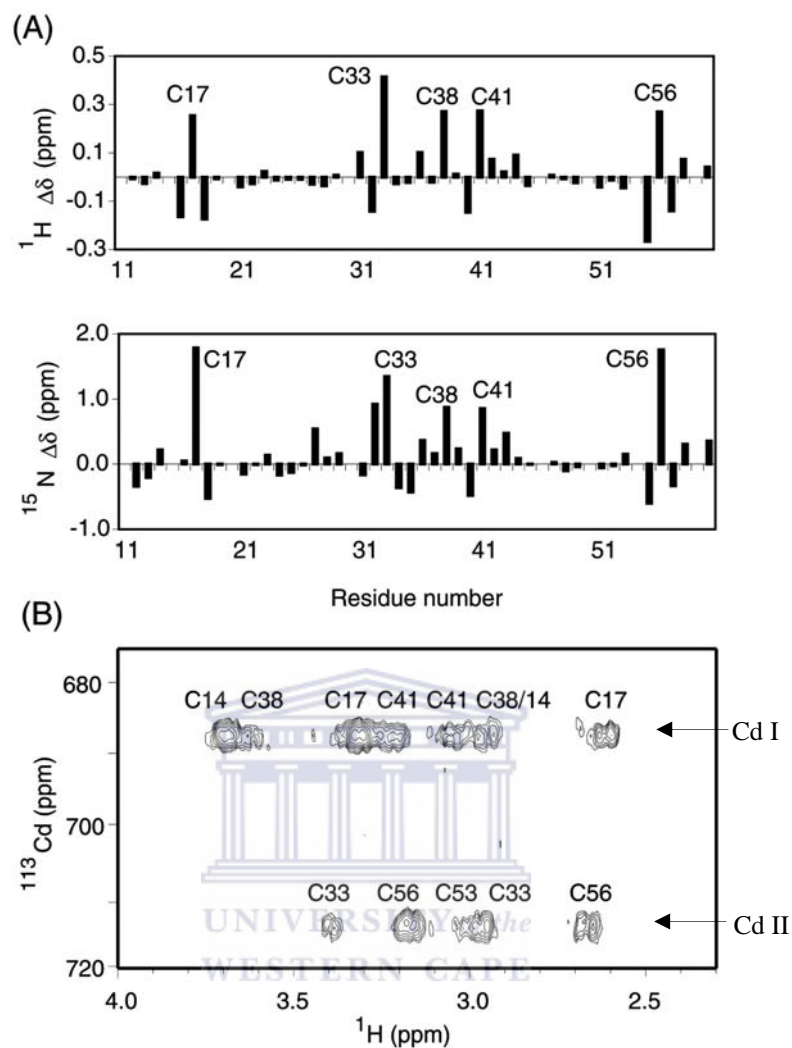


Figure 1.12 Determination of zinc coordinating residues by replacement of zinc with ^{113}Cd in the CNOT4 RING domain. Chemical shift differences of the amide protons and nitrogen's between native Zn-bound CNOT4 and the Cd-bound CNOT4 are shown in (A). ^{113}Cd - ^1H HSQC spectrum (B) shows the correlation between ^{113}Cd and H^β protons of the cysteine residues. Site 1 contains residues Cys 14, 17, 38, and 41 and site 2 contains residues Cys 33, 53, and 56. H^β protons for cysteine residues have chemical shifts in the vicinity of 2.5-4.0 ppm (figure adapted from Hanzawa *et al.*, 2001).

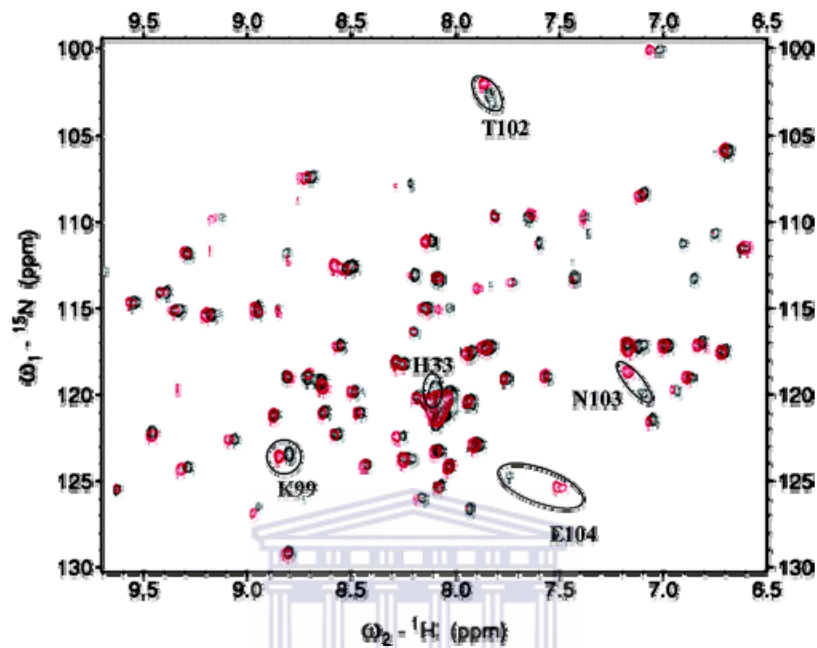


Figure 1.13 Zn^{2+} or Cd^{2+} binding in oxidised Cytochrome *c*. ^{15}N -HSQC of Cytochrome *c*, before (red) and after (black) the addition of Zn^{2+} . Chemical shift changes were observed for E104, N103, T102, H33 and K99. The shifts are only observed for a small number of residues meaning that binding of Zn^{2+} has no effect on the integrity of the whole protein (figure adapted from Gourion-Arsiquaud *et al.*, 2005).

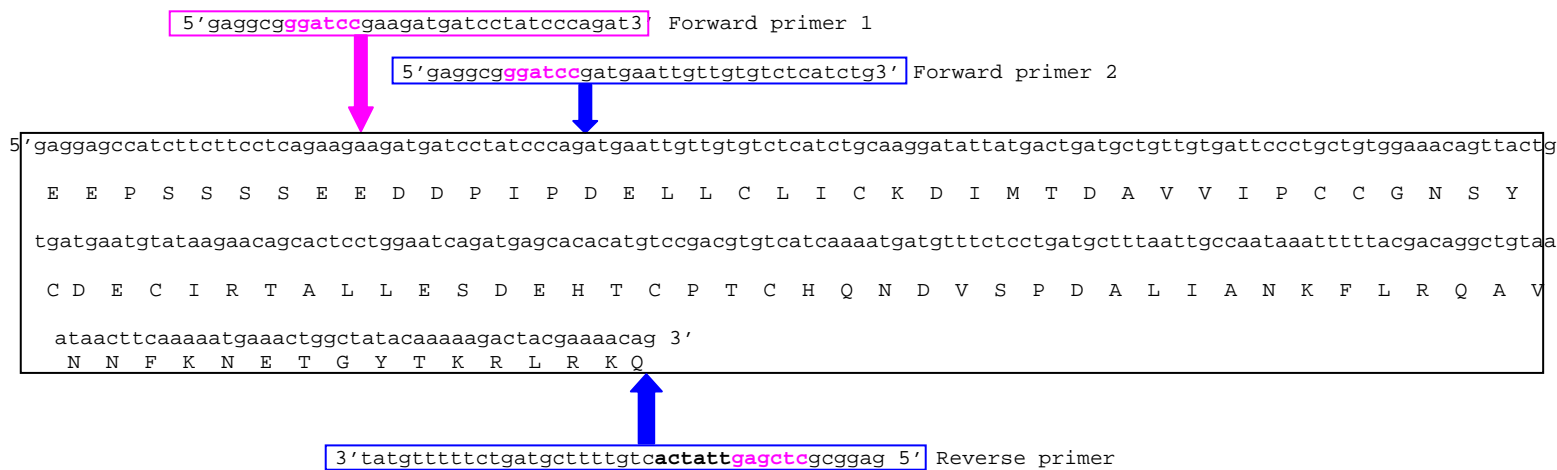
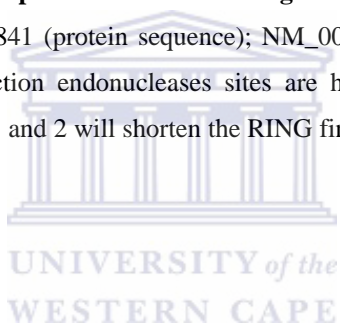


Figure 3.1 Primers used for PCR amplification of RING finger. The sequence is taken from the human RBBP6 (Accession number NP_008841 (protein sequence); NM_006910 (nucleotide sequence), residues 249-335). *Bam* HI and *Xho* I restriction endonucleases sites are highlighted in pink. Stop codons are highlighted in bold. Forward primer 1 and 2 will shorten the RING finger by 13 and 19 amino acid residues respectively.



QuickTime™ and a
TIFF (LZW) decompressor
are needed to see this picture.



Figure 3.2 1% agarose gel electrophoresis showing PCR amplification of both shortened RING constructs. Lanes 2 and 3 correspond to RING_{ss} and RING_{sl} respectively. Lane 1 corresponds to the negative control (no DNA template) and lane M corresponds to a Mass ruler DNA ladder marker. RING_{ss} was shortened by 57 base pairs (19 amino acids) giving a size of 243 bp, and RING_{sl} was shortened by 39 base pairs (13 amino acids) giving a size of 261 bp.

QuickTime™ and a
TIFF (LZW) decompressor
are needed to see this picture.

Figure 3.3 1% agarose gel electrophoresis showing colony PCR screening for recombinant clones. Lanes 3-7 correspond to RING_sl, lanes 8-11 correspond to RING_ss. The expected sizes for positive clones are 461 and 443 respectively. Positive clones for RING_sl are in lanes 3,4,6; lane 8 contains a single positive RING_ss clone. Negative clones are in lanes 5,7, 9-11. Lane 1 is the negative control (no DNA template), lane 2 contains a positive control for the PCR reaction for which the template was pGEM-DWNN from (*Encephalitozoon cuniculi*), lane M corresponds to pTZ marker.



pGEM-T easy

RING sl

Figure 3.4 1% agarose gel electrophoresis showing restriction digestion of pGEM-T Easy-RING shortened constructs with *Bam* HI and *Xho* I. Lanes 1 & 2 correspond to undigested and digested pGEM-T Easy RING_ss respectively. Lanes 3 & 4 correspond to undigested and digested pGEM-T Easy-RING_sl respectively. Lane M corresponds to the Mass ruler DNA ladder marker. The expected size for the released insert in lane 4 is 261 bp.

QuickTime™ and a
TIFF (LZW) decompressor
are needed to see this picture.

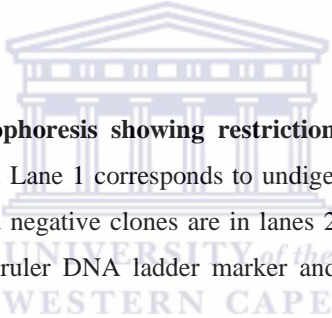


Figure 3.5 1% agarose gel electrophoresis showing restriction digestion of pGEX-6P-2-RING_sl constructs with *Bam* HI and *Xho* I. Lane 1 corresponds to undigested plasmid, lanes 2-9 correspond to digested plasmid. Positive clones and negative clones are in lanes 2-4 & 6 and lanes 5, 7-9 respectively. Lane M (left) corresponds to Mass ruler DNA ladder marker and lane M (right) corresponds to pTZ marker.

QuickTime™ and a
TIFF (LZW) decompressor
are needed to see this picture.

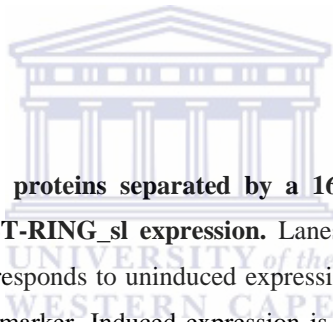


Figure 3.6 Coomassie Blue stained proteins separated by a 16% SDS PAGE gel electrophoresis showing small-scale screen for GST-RING_sl expression. Lanes 1, 3, 5 & 7 correspond to induced expression and lanes 2, 4, 6 & 8 corresponds to uninduced expression. Lane 9 contains GST, and lane M contains a protein molecular weight marker. Induced expression is characterised by a prominent band at ~36.8 kD, which is not present in the uninduced lanes.

A

QuickTime™ and a
TIFF (LZW) decompressor
are needed to see this picture.

B



Figure 3.7 Large-scale expression and affinity purification of GST-RING_sl and its separation from GST by 3C protease. In (A) RING_sl was expressed in minimal media in the presence of 100 μ M ZnSO₄. Lane 1 corresponds to the lysate, lane 2 corresponds to the flow through, lane 3-5 correspond to the 1st wash, 2nd wash, and 3rd wash respectively. Lanes 6-7 each corresponds to GST-RING_sl protein. Lane 8 corresponds to the NaCl wash. Purified GST-RING_sl was cleaved (B) using 3C protease and GST was removed by the second round of glutathione agarose chromatography. Lane 1: uncleaved GST-RING_sl, lane 2: cleaved GST-RING_sl, lane 3 flow through containing RING_sl, lane 4: wash, lane 5 & 6 eluted GST. RING_sl has an apparent molecular weight of 14-20 kD when visualised on an SDS PAGE gel, suggesting that is partially dimeric. Lane M corresponds to the protein molecular weight marker.

A

QuickTime™ and a
TIFF (LZW) decompressor
are needed to see this picture.

B



Figure 3.8 Removal of residual GST from RING_sl by anion exchange chromatography. (A) Peak 1 corresponds to the flow through, Peak 2 to RING_sl, and Peak 3 to GST. (B) SDS PAGE gel of fractions from the chromatogram. Lane 1 corresponds to RING_sl before anion exchange chromatography, lane 2 corresponds to the fraction in Peak 2. Lane 5 corresponds to the fraction in Peak 3. Lane M is the protein molecular weight marker.

A

QuickTime™ and a
TIFF (LZW) decompressor
are needed to see this picture.

B



Figure 3.9 Removal of residual GST and small molecules from RING_sl by size exclusion chromatography. (A) Peak 1 corresponds to GST and peak 2 to RING_sl. A clear separation of GST and RING_sl was achieved. (B) SDS PAGE gel of fractions from the chromatography. Lane 1 corresponds to the void volume and lanes 2&3 correspond to peak 1 (GST). Lanes 4-8 correspond to peak 2 (RING_sl). Lane M corresponds to the protein molecular weight marker. Note that RING_sl consistently shows an apparent molecular weight consistent with it being a dimer, despite the presence of 1 mM DTT.

A

QuickTime™ and a
TIFF (LZW) decompressor
are needed to see this picture.

B



Figure 3.10 Removal of residual GST and small molecules from purified RING_{ss} domain by size exclusion chromatography. (A) Peak 1 corresponds to proteins with high molecular weight, peak 2 to GST and peak 3 to RING_{ss}. A clear separation of GST and RING_{ss} was achieved. (B) SDS PAGE gel of fractions from the chromatography. Lane 1 corresponds to the void volume (peak 1), lane 2 corresponds to peak 2 (GST), Lanes 4-8 correspond to peak 3 (RING_{ss}). Lane 9 corresponds to RING_{ss} before putting it on the gel filtration column, and lane M corresponds to the protein molecular weight marker. The gel reveals that after gel filtration RING_{ss} still appears to be monomeric (~14.4 and 10.0 kD).

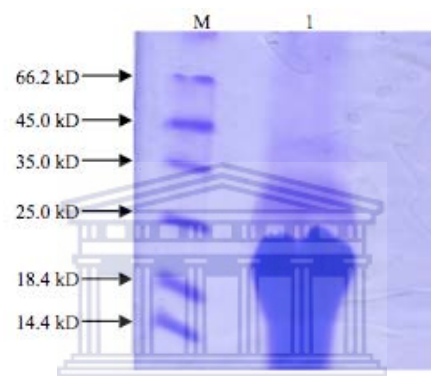


Figure 3.11 Coomassie Blue stained proteins analysed using 16 % SDS PAGE gel electrophoresis showing the final concentrated RING_sl in 5 mM DTT. Lane 1 corresponds to concentrated RING_sl, and lane M corresponds to the protein molecular weight marker.

Table 3.1 Absorbance of the Bradford reagent measured at 595 nm for the standard protein (BSA) and RING_sl.

Concentration of standard protein ($\mu\text{g/ml}$)	Absorbance of standard protein (595 nm)
0	0
10	0.172
20	0.403
30	0.544
40	0.637
50	0.776
Dilutions for RING_sl	Abs for RING_sl
1:1000	0.4685
1:2000	0.237

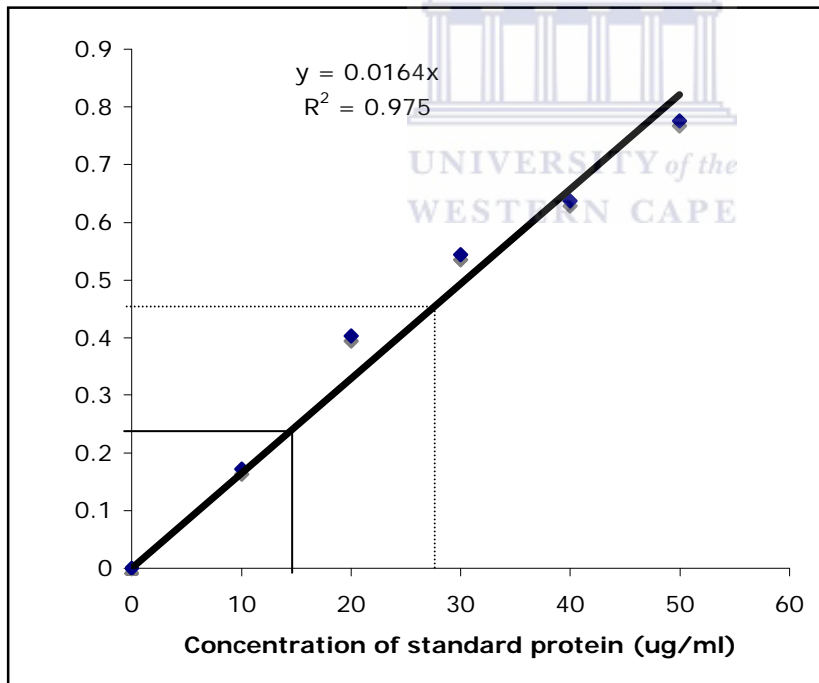


Figure 3.12 Bradford Assay standard curve for quantifying the concentration of RING_sl. A_{595} values of the standard protein (BSA) concentrations are plotted against different concentrations. The unknown concentration of RING_sl is determined using the measured absorbance values at two different dilutions. The dashed and continuous lines correspond to 1:1000 and 1:2000 dilutions respectively. The values corresponding to the concentration are calculated using the formula corresponding to the straight line fitted to the data.

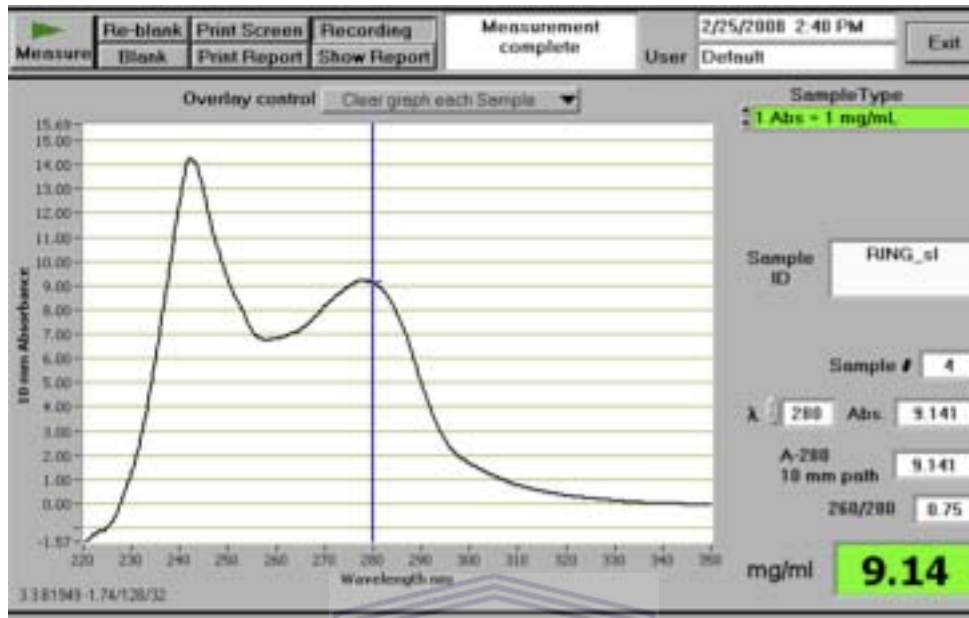


Figure 3.13 UV absorption spectrum of RING_sl protein determined using NanoDrop spectrometer. The large broad peak at 280 nm indicates the amount of protein available, and the absorbance value of 9.14, measured at an optical path length of 10 mm.

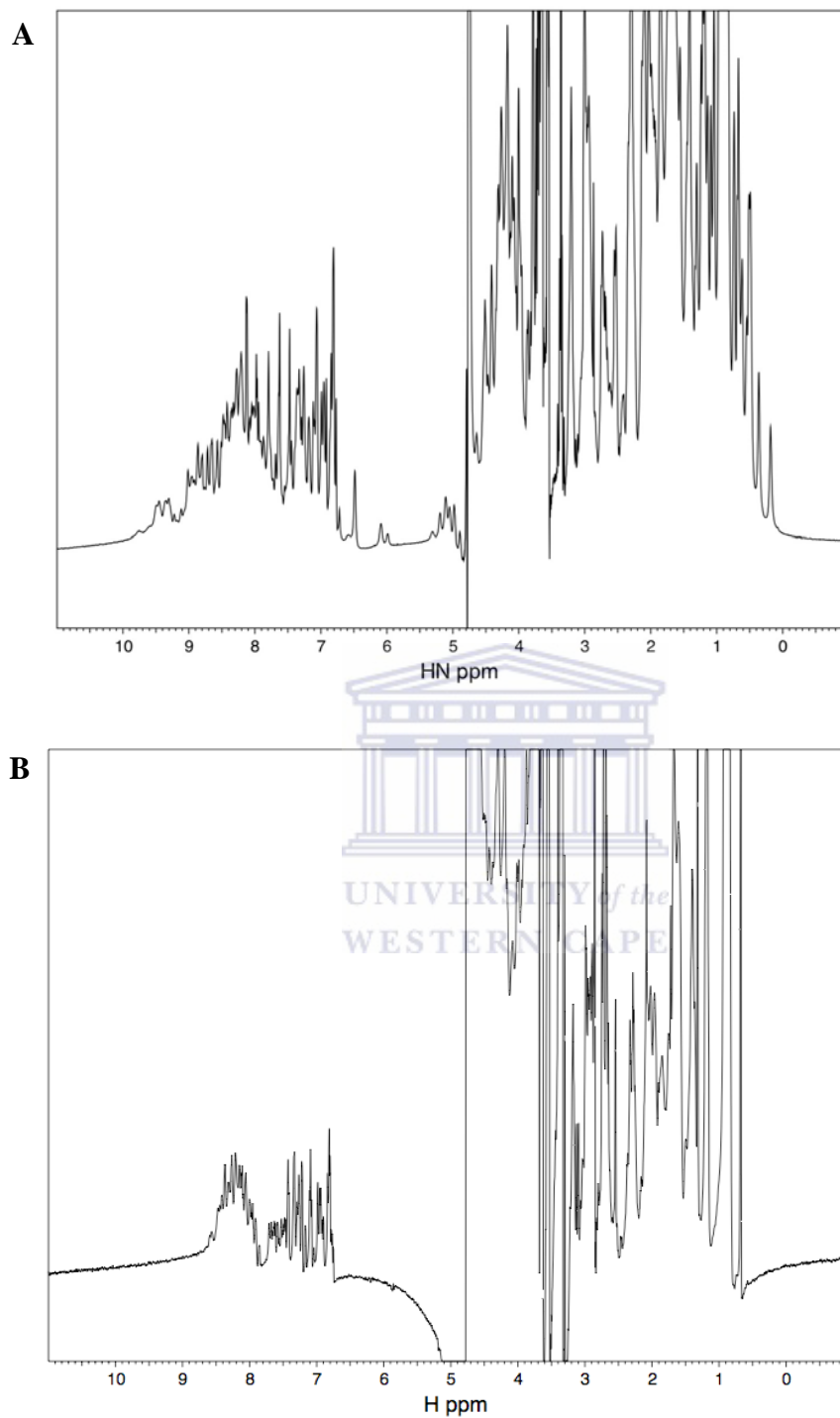


Figure 4.1 1D spectra of shortened RING constructs, pH6.0, 25 °C, recorded at 600 MHz. **A** is the RING_sl and **B** is the RING_ss. In (A) the appearance of the resonances aromatic in the region (9-7.5 ppm), α -protons in the region (7.5- 4.5 ppm), β -protons region (4.5-3.5 ppm), and methyl protons in the region (3.5-0 ppm) indicate that RING_sl is folded. In (B) the absence of the α -protons in the regions 7.5- 4.5 ppm, and the methyl protons in the region between 1-0 ppm indicate that RING_ss is unfolded.

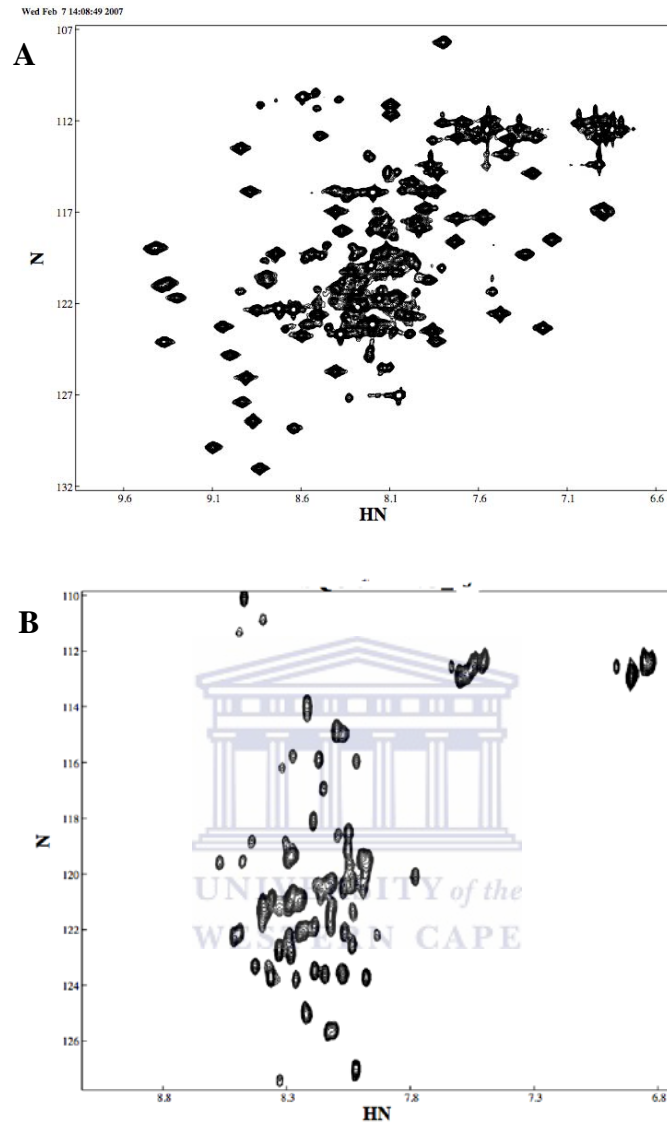


Figure 4.2 ^{15}N -HSQC spectra of RING constructs, pH 6.0, 25 °C, recorded at 600 MHz. **A** is the RING_sl and **B** is the RING_ss. (A) ^{15}N -HSQC spectrum for RING_sl, the resonances are sharp and well dispersed in both dimensions, which is characteristic of folded proteins. There are also more peaks. The NH_2 groups at the top right are also well dispersed. (B) ^{15}N -HSQC spectrum for RING_ss, the resonances are broad and poorly dispersed in the H^{N} dimension, which is characteristic of unfolded proteins. The NH_2 groups at top right are also poorly dispersed.

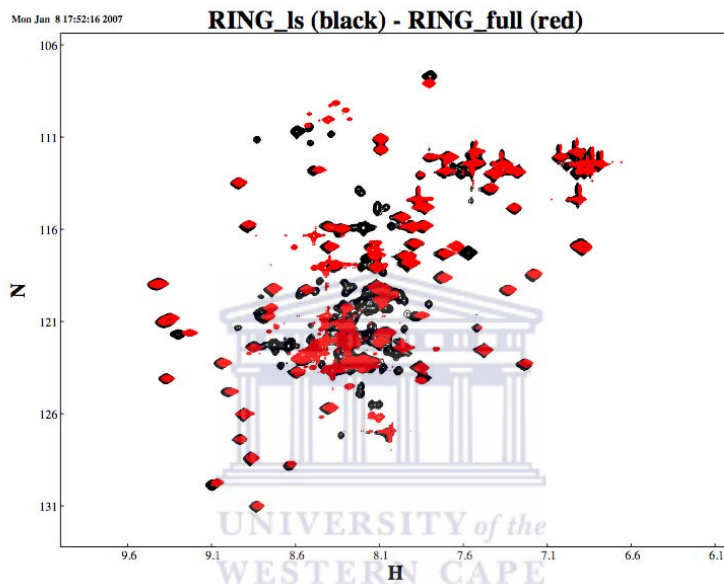


Figure 4.3 Overlay ^{15}N -HSQC spectra of RING_sl (black) domain and previous RING full (red) constructs, pH 6.0, 25 °C, recorded at 600 MHz. As shown RING_sl and the previous construct are well folded since the signals are well dispersed on both dimensions. The spectrum shows that RING_sl adopts the same structure as the previous RING construct.

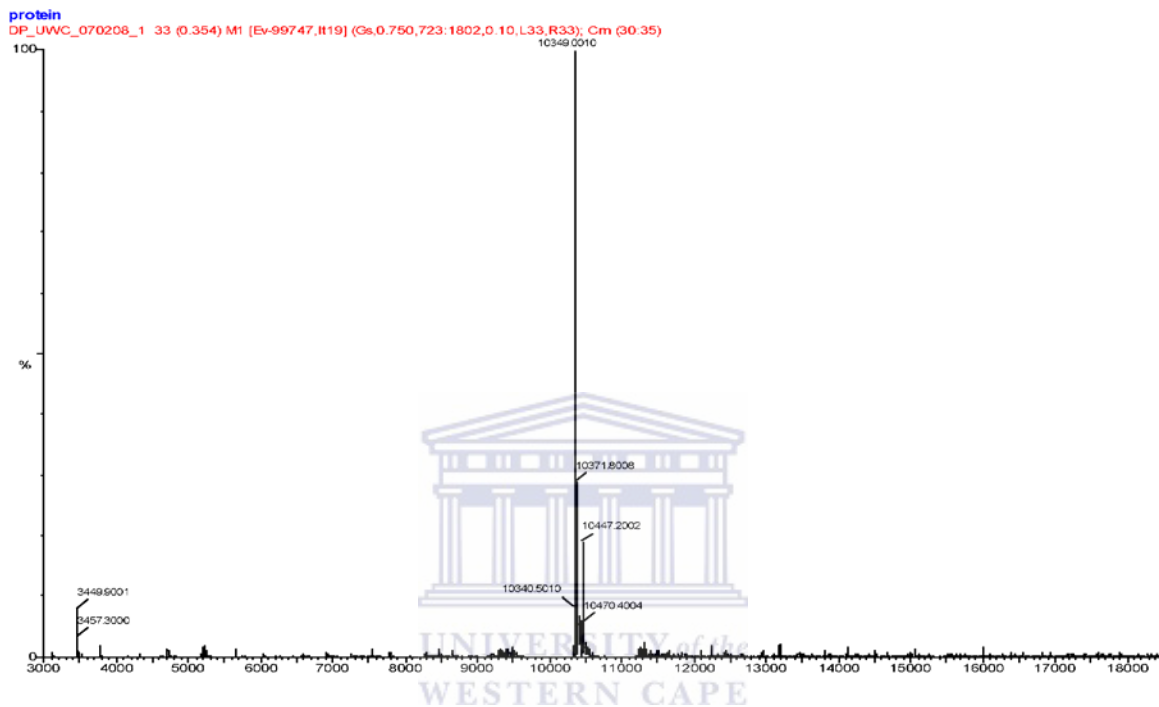


Figure 4.4 Determination of molecular mass of RING_sl using mass spectrometer. The expected mass for RING_sl is 10229.6, for ^{15}N -labelled RING_sl is 10351.6 Da, since 122 Da is added to every nitrogen, and for, Zn^{2+} bound ^{15}N -labelled RING_sl is 10417.009 Da if one Zn^{2+} is bound and 10482.418 Da if two Zn^{2+} are bound. The results show the mass of the protein without any Zn^{2+} bound, corresponding to 10349.00 Da.

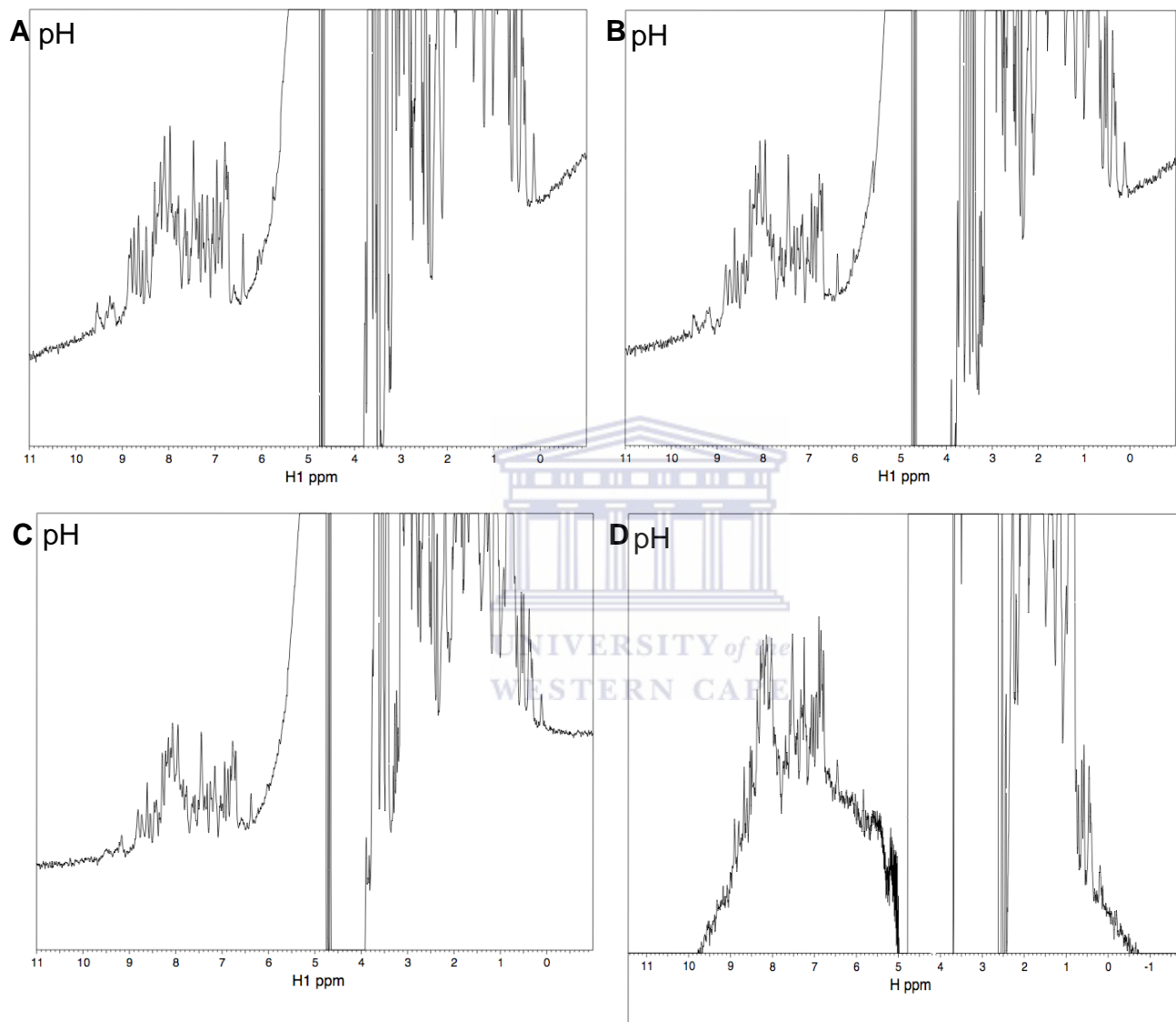


Figure 4.5 1D spectra of RING_sl at different pH conditions. Unlabelled RING_sl sample was prepared in five different pH buffers (A) pH 6.0, (B) pH 5.8, (C) pH 5.6, and (D) pH 5.2. The protein starts to unfold at pH 5.6 as shown by the disappearance of resonances between 9 and 6 ppm and at 0.1 ppm. By pH 5.2 RING_sl is almost completely unfolded.

QuickTime™ and a
TIFF (LZW) decompressor
are needed to see this picture.



Figure 4.6 Separation of the unfolded/aggregated protein from the folded protein and the removal of excess Cadmium/Zinc to determine the stability of Cadmium/Zinc in RING_sl using size exclusion chromatography. Peak 1 and peak 2 correspond to RING_sl. SDS PAGE gel analysis confirms that both peaks contain RING_sl protein. Lane 1,2,3, and 4 contain fractions that correspond to the broad peak, and lanes 5 to 8 contain fractions that correspond to the narrow peak, lane 9 is the protein before gel filtration purification. M correspond to the protein molecular weight marker.

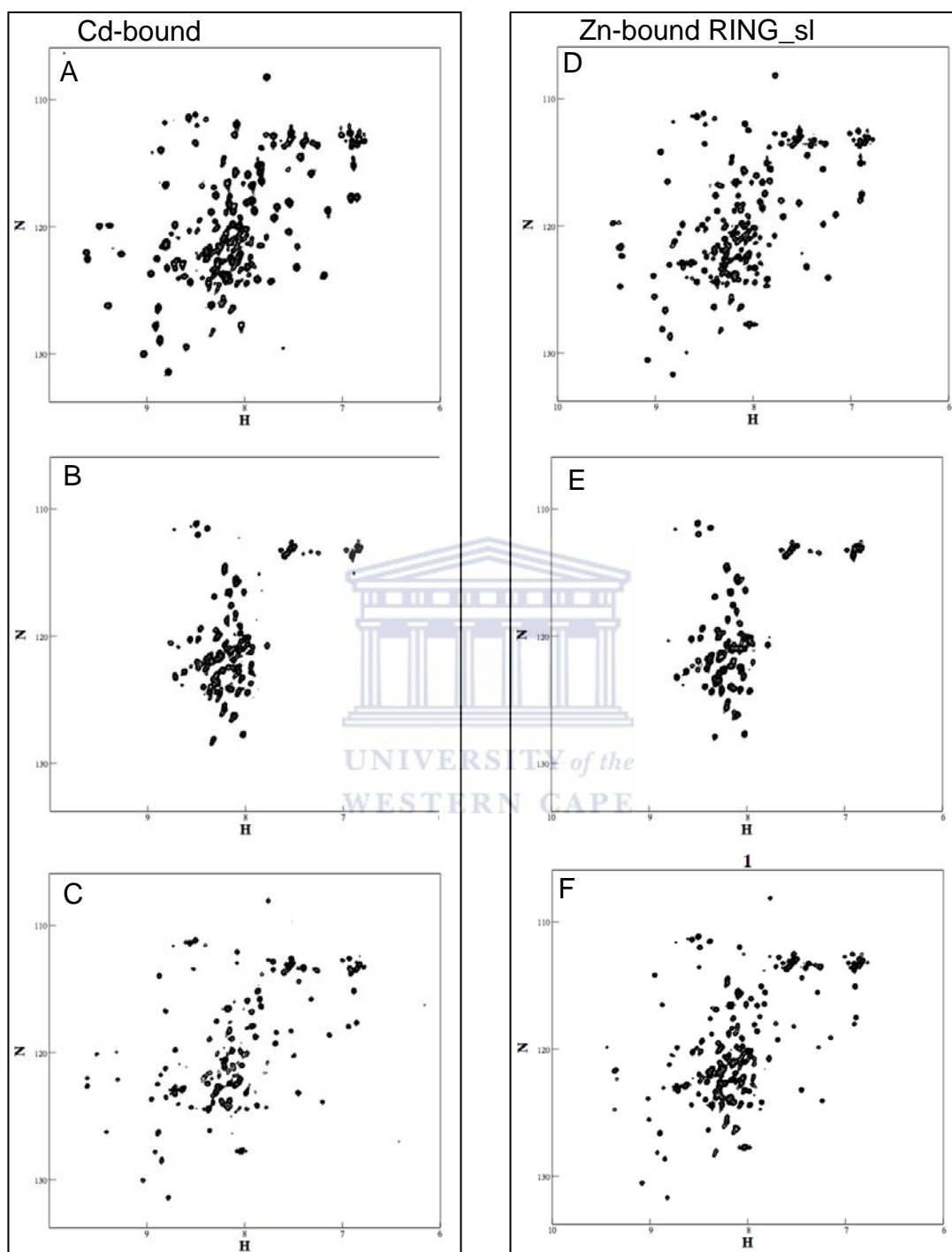


Figure 4.7 ^{15}N -HSQC spectra of RING_sl, pH 6.0, 25 °C, recorded at 600 MHz, showing the removal of excess cadmium/zinc, and aggregated protein using size exclusion chromatography. After purification the chromatogram contained the sharp peak corresponding to spectrum in (A & D), and the broad peak corresponding to (B & E). CdCl_2 / ZnCl_2 was added to the unfolded protein (broad peak) giving a spectrum in (C & F) in which the protein has refolded.

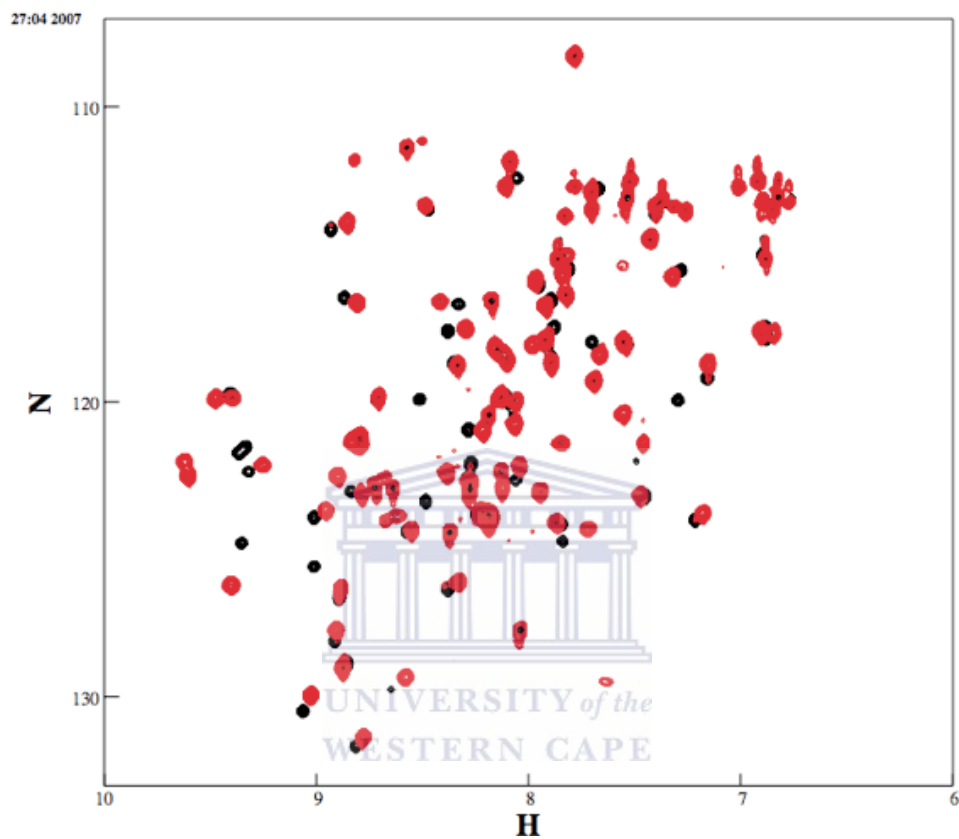


Figure 4.8 Superimposition of ¹⁵N-HSQC spectra of RING_sl, pH 6.0, 25 °C, recorded at 600 MHz, before (black) and 2 weeks after (red) the addition of 2 mM ¹¹³Cd-EDTA. Some resonances have shifted after the addition of ¹¹³Cd-EDTA, indicating that exchange has taken place.

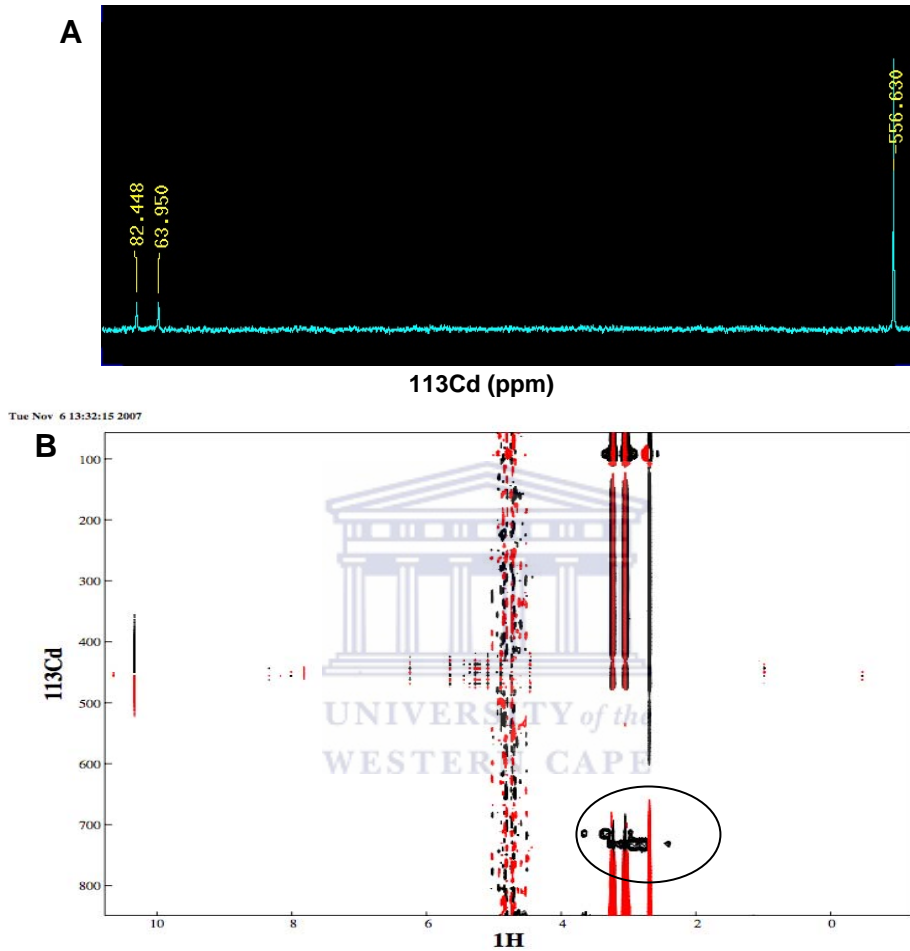


Figure 4.9 Cadmium- zinc exchange experiments monitored by 1D directly detected and correlation experiments. (A) 1D directly detected ^{113}Cd spectrum of RING_sl in the presence of ^{113}Cd -EDTA. The resonance at 556.630 corresponds to ^{113}Cd -EDTA and the two resonances at 82.448 and 63.950 to the two ^{113}Cd ions bound to the protein. (B) ^{113}Cd -HSQC spectra of RING_sl in the presence of ^{113}Cd -EDTA. The projection of the ^{113}Cd -HSQC on the right hand side is the same as the 1D directly detected spectrum (A).

Tue Nov 6 13:42:33 2007

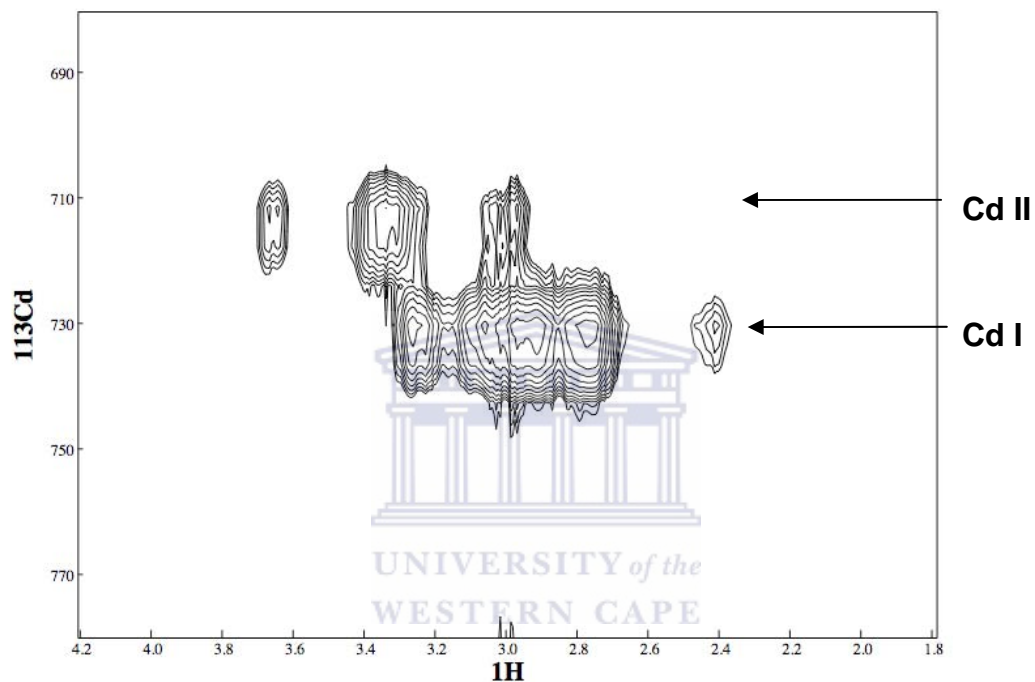


Figure 4.10 ^{113}Cd -HSQC spectrum of the cadmium-exchanged RING_sl. Expanded form of 4.9B (circled), showing two lines of peaks, each representing correlation transfer between one of the $^{113}\text{Cd}^{2+}$ ions and the H^{β} protons of the coordinating cysteines residues.